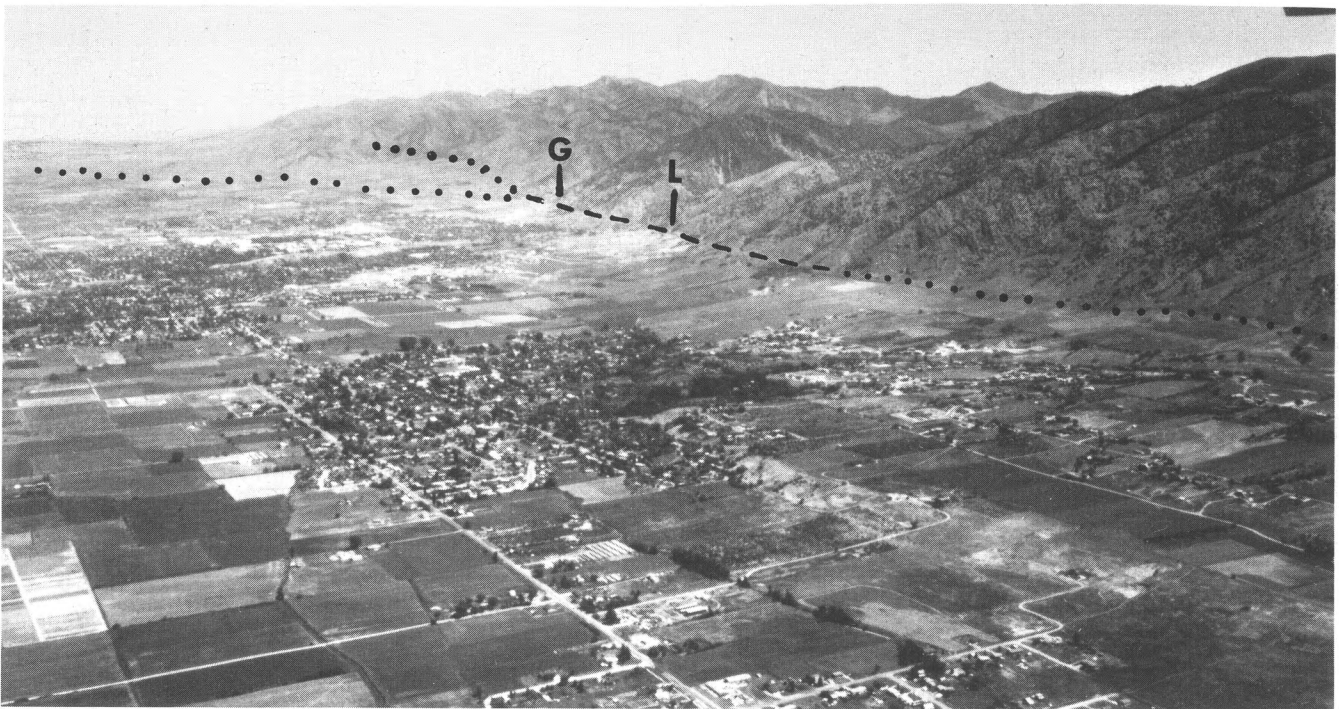


Paleoseismology of Utah, Volume 5

**NEOTECTONIC DEFORMATION ALONG
THE EAST CACHE FAULT ZONE,
CACHE COUNTY, UTAH**

by
James P. McCalpin
Department of Geology
Utah State University



STATE OF UTAH
Michael O. Leavitt, Governor

DEPARTMENT OF NATURAL RESOURCES
Ted Stewart, Executive Director

UTAH GEOLOGICAL SURVEY
M. Lee Allison, Director

UGS Board

<u>Member</u>	<u>Representing</u>
Russell C. Babcock, Jr. (chairman)	Mineral Industry
Lynnelle G. Eckels	Mineral Industry
Richard R. Kennedy	Civil Engineering
Jo Brandt	Public-at-Large
C. William Berge	Mineral Industry
Jerry Golden	Mineral Industry
Milton E. Wadsworth	Economics-Business/Scientific
Scott Hirschi, Director, Division of State Lands and Forestry	Ex officio member

UGS Editorial Staff

J. Stringfellow	Editor
Vicky Clarke, Sharon Hamre	Editorial Staff
Patricia H. Speranza, James W. Parker, Lori Douglas	Cartographers

UTAH GEOLOGICAL SURVEY
2363 South Foothill Drive
Salt Lake City, Utah 84109-1491

THE UTAH GEOLOGICAL SURVEY is organized into three geologic programs with Administration, Editorial, and Computer Resources providing necessary support to the programs. THE ECONOMIC GEOLOGY PROGRAM undertakes studies to identify coal, geothermal, uranium, hydrocarbon, and industrial and metallic mineral resources; to initiate detailed studies of the above resources including mining district and field studies; to develop computerized resource data bases, to answer state, federal, and industry requests for information; and to encourage the prudent development of Utah's geologic resources. THE APPLIED GEOLOGY PROGRAM responds to requests from local and state governmental entities for engineering geologic investigations; and identifies, documents, and interprets Utah's geologic hazards. THE GEOLOGIC MAPPING PROGRAM maps the bedrock and surficial geology of the state at a regional scale by county and at a more detailed scale by quadrangle. The Geologic Extension Service answers inquiries from the public and provides information about Utah's geology in a non-technical format.

The UGS manages a library which is open to the public and contains many reference works on Utah geology and many unpublished documents on aspects of Utah geology by UGS staff and others. The UGS has begun several computer data bases with information on mineral and energy resources, geologic hazards, stratigraphic sections, and bibliographic references. Most files may be viewed by using the UGS Library. The UGS also manages a sample library which contains core, cuttings, and soil samples from mineral and petroleum drill holes and engineering geology investigations. Samples may be viewed at the Sample Library or requested as a loan for outside study.

The UGS publishes the results of its investigations in the form of maps, reports, and compilations of data that are accessible to the public. For information on UGS publications, contact the UGS Sales Office, 2363 South Foothill Drive, Salt Lake City, Utah 84109-1491, (801) 467-7970.

The Utah Department of Natural Resources receives federal aid and prohibits discrimination on the basis of race, color, sex, age, national origin, or handicap. For information or complaints regarding discrimination, contact Executive Director, Utah Department of Natural Resources, 1636 West North Temple #316, Salt Lake City, UT 84116-3193 or Office of Equal Opportunity, U.S. Department of the Interior, Washington, DC 20240.



Printed on recycled paper

FOREWORD

This Utah Geological Survey Special Study "Neotectonic Deformation Along the East Cache Fault Zone, Cache County, Utah" is the fifth report in the "Paleoseismology of Utah" Special Studies series. The purpose of the series is to make the results of paleoseismic investigations in Utah available to geologists, engineers, public planners and decision makers, and the general public. These studies provide critical information on earthquake timing, recurrence, displacement, slip rate, and fault geometry which is used to characterize the long-term earthquake potential (hazard) and risk from Quaternary faults.

The East Cache fault zone trends along the east side of northern Utah's Cache Valley, at the base of the precipitous Bear River Range. Fault scarps in geologically young deposits (latest Pleistocene and Holocene) and well-developed faceted spurs along the range front have long indicated to geologists the active nature of this fault. In this report, Dr. James P. McCalpin, Research Associate Professor at Utah State University and President of GEO-HAZ Consulting, uses the results from two detailed trenching investigations, an evaluation of Bonneville-highstand shoreline deformation, and geomorphic analysis of Bear River Range front faceted spurs to characterize the prehistoric seismic behavior and the earthquake potential of the East Cache fault zone. Much of the initial funding for this study was provided by the U.S. Geological Survey as part of their National Earthquake Hazard Research Program. Funding to prepare this report for publication was provided through the UGS Mineral Lease Special Projects Program.

William R. Lund, Series Editor
Utah Geological Survey

also in the Paleoseismology of Utah Special Studies Series

Utah Geological Survey Special Study 75, 1991, Paleoseismology of Utah, Volume 1: Fault behavior and earthquake recurrence on the Provo segment of the Wasatch fault zone at Mapleton, Utah County, Utah by W.R. Lund, D.P. Schwartz, W.E. Mulvey, K.E. Budding, and B.D. Black.

Utah Geological Survey Special Study 76, 1991, Paleoseismology of Utah, Volume 2: Paleoseismic analysis of the Wasatch fault zone at the Brigham City trench site, Brigham City, Utah and the Pole Patch trench site, Pleasant View, Utah by S.F. Personius.

Utah Geological Survey Special Study 78, 1991, Paleoseismology of Utah, Volume 3: The number and timing of Holocene paleoseismic events on the Nephi and Levan segments of the Wasatch fault zone, Utah by Michael Jackson.

Utah Geological Survey Special Study 82, 1994, Paleoseismology of Utah, Volume 4: Seismotectonics of north-central Utah and southwestern Wyoming by Michael W. West.

Paleoseismology of Utah, Volume 5

**NEOTECTONIC DEFORMATION ALONG
THE EAST CACHE FAULT ZONE,
CACHE COUNTY, UTAH**

by
James P. McCalpin
Department of Geology
Utah State University

Special Study 83
UTAH GEOLOGICAL SURVEY
a division of
UTAH DEPARTMENT OF NATURAL RESOURCES

1994



**THE PUBLICATION OF THIS PAPER
IS MADE POSSIBLE WITH MINERAL LEASE FUNDS**

No endorsement of specific products or firms named in this publication is intended by the Utah Geological Survey, nor is criticism implied of those not mentioned.

Articles and information appearing in this publication become public property upon publication release.

Duplication is encouraged, with recognition of author and source, provided that no endorsement of a specific commercial product, firm, or concept is stated or implied.

A primary mission of the UGS is to provide geologic information of Utah through publications; the formal publication series is reserved for material whose senior author is a UGS staff member. This Mineral Lease publication provides an outlet for non-UGS authors without necessarily going through extensive policy, technical, and editorial review required by the formal series. It also provides a means for non-UGS authors to publish more interpretive work with the knowledge that readers will exercise some degree of caution.

This publication is printed on recycled paper.

CONTENTS

Abstract	1
Introduction	2
Surficial Geologic Mapping	2
Quaternary Faulting and Segmentation of the East Cache fault zone	3
Northern Section	4
Slip Rate and Recurrence	6
Central Section	6
The Bonneville Trench	9
Numerical Ages	10
Chronology of Faulting	10
The Provo Trench	14
Hidden Fault Traces	16
Summary of Paleoseismology of the Central Section	16
Southern Section	17
Slip rates and Recurrence	18
Paleoearthquake magnitudes	18
Deformation of the Bonneville Highstand Shoreline	19
Methods	20
Results	23
Longitudinal Profile	23
Transverse Profile	24
Tectonic Geomorphology of the Bear River Range Front	26
Overall Physiography	26
Faceted Spurs	26
Methods	26
Results	26
Drainage Basin Analysis	29
Conclusions	31
Acknowledgments	31
References	32
Appendix 1; Unit Descriptions, Bonneville Trench	35
Appendix 2; Unit Descriptions, Provo Trench	37

ILLUSTRATIONS

Figure 1. Location map of the study area	2
Figure 2. Oblique aerial photograph of the Bear River Range front	3
Figure 3. Map of the East Cache fault zone	4
Figure 4. Sketch of multiple faults in a gravel pit wall	5
Figure 5. Surficial geologic map of the area near the mouth of Logan Canyon	7
Figure 6. Photograph and sketch of U.S. Highway 89 road cut at the mouth of Logan Canyon	8
Figure 7. Photograph of the trace of the ECFZ	9
Figure 8. Log of the Bonneville trench across the central section of the ECFZ	11
Figure 9. Photograph of the main fault zone in the Bonneville trench	12
Figure 10. Photograph of the fault scarp traversing the post-Provo strath terrace	15
Figure 11. Log of the Provo trench across the central section of the ECFZ	15
Figure 12. Sketch of “hidden” fault exposed in a landslide near the Utah State University campus	16
Figure 13. Diagram of inferred timing of faulting events, central section ECFZ	17
Figure 14. Sketches of fault traces on the southern section of the ECFZ	19
Figure 15. Longitudinal profile of the Bonneville highstand shoreline	23
Figure 16. Transverse profile of the elevations of the highstand shoreline of the Bonneville lake cycle	25

Figure 17. Photograph of faceted spurs along the Bear River Range front east of Providence, Utah	27
Figure 18. Diagram of faceted spurs along the Bear River Range front	28
Figure 19. Frequency histograms of drainage basin parameters for drainage basins intersecting the ECFZ	30

TABLES

Table 1. Fault scarp profile data	10
Table 2. Vertical displacements on individual faults, Bonneville trench	12
Table 3. Quantitative soil data, Bonneville trench	14
Table 4. Inferred magnitudes of paleoearthquakes on the central section of the ECFZ	20
Table 5. Summary of control data for survey traverses, Bonneville highstand shoreline	21
Table 6. Comparison of the closed traverse <i>vs</i> the radial sight method	22
Table 7. Input data for rheologic modeling of Bonneville highstand shoreline deformation	25

Paleoseismology of Utah, Volume 5

NEOTECTONIC DEFORMATION ALONG THE EAST CACHE FAULT ZONE, CACHE COUNTY, UTAH

by
James P. McCalpin
Department of Geology
Utah State University
*Logan, UT 84322-4505**

ABSTRACT

The Quaternary history of the East Cache fault zone was investigated utilizing surficial geologic mapping, backhoe trenching of fault scarps, surveying the Bonneville highstand shoreline, and measuring quantitative geomorphology of the Bear River Range front. Fault scarps displace deposits of the Bonneville lake cycle and younger sediments for 8 kilometers (4.8 mi) along an area east of Logan, Utah. To the north and south, the less youthful appearing range front either shows no clear evidence of late Quaternary faulting, or exhibits only pre-Bonneville-lake-cycle faults in rare exposures.

Based on geomorphology and age of latest faulting, the fault is divisible into a northern section greater than 26 kilometers (>15.6 mi) long, a central section 16 kilometers (9.6 mi) long (with post-Bonneville fault scarps), and a southern section greater than 14 kilometers (>8.4 mi) long. The northern section appears to have been the least active in the late Quaternary, and no fault scarps were found across any late Quaternary surfaces in that section. An apparent 20-meter (65.6 ft) displacement of a pre-Bonneville pediment at the southern end of the northern section implies a long-term slip rate of only about 0.05-0.10 mm/yr (0.002-0.004 in/yr). In contrast, two surface-faulting events have occurred in the central section since occupation of the Bonneville highstand shoreline (15.5 thousand years ago). Radiocarbon and thermoluminescence (TL) age estimates, and quantitative pedology from two trenches, suggest the earlier event (displacement 1.4-1.9 m; 4.6-6.2 ft) occurred between 13 and 15.5 thousand years ago, and a later event (displacement 0.5 m-1.2 m; 1.6-3.9 ft) occurred about 4 thousand years ago. Evidence for an event earlier during the Bonneville transgression is equivocal. Long-term slip rates based on an 8.5 meter (27.9 ft) displacement of pre-Bonneville alluvium are as high as 0.06

mm/yr (0.002 in/yr), depending on age of the alluvium. Quaternary faults also occur on the southern section, but TL age estimates indicate that latest faulting occurred between about 26 and 46 thousand years ago. Long-term slip rates based on pediment offsets may be as high as 0.07 mm/yr (0.003 in/yr).

The elevation of the Bonneville highstand shoreline was surveyed at 82 locations along the East Cache fault zone to an accuracy of roughly 1 meter (3.3 ft), but surveying revealed no discrete displacements where the shoreline crossed inferred fault segment boundaries. There was no elevation difference between reaches where post-Bonneville faulting of up to 4.2 meters (13.8 ft) had occurred, and reaches where no faulting had occurred. However, three elevation downwarps (amplitudes of 2.5-5.3 m; 8.2-17.4 ft) occurred spatially coincident with large Bonneville/Provo delta complexes. The crust underneath Cache Valley was rheologically modeled as a beam subjected to point depositional loading by the deltaic piles. Model results show that the amplitude of the shoreline elevation anomalies can be predicted assuming reasonable deltaic weights and crustal strength parameters, but the observed radii of deformation are much smaller than predicted.

The unique faceted spur structure of the central segment extends across section boundaries to the north and south, indicating that, in a long-term sense, uplift events may not have terminated at present segment boundaries. Though ambiguous, facet spacing and pattern suggest that the western splay fault of the northern section has developed recently, transferring displacement away from the eastern splay. In contrast, young facets of the central segment extend through the southern section on the eastern splay, suggesting that some Quaternary rupture events may involve both sections (combined length >29 km; >17 mi).

*current address: GEO-HAZ Consulting, P.O. Box 1377, Estes Park, CO 80517

INTRODUCTION

Cache Valley is a major intermontane graben east of the Wasatch fault zone in northern Utah and southeastern Idaho (figure 1). The valley (average elevation 1,370 m; 4,493 ft) is flanked on the west by the Wellsville Mountains (maximum elevation 2,860 m; 9,380 ft) and on the east by the Bear River Range (maximum elevation 3,042 m; 9,978 ft). Valley length is about 80 kilometers (48 mi) and width varies from 13 kilometers (7.8 mi) at the southern end to 20 kilometers (12 mi) at the latitude of Logan, Utah. The flanking mountain ranges are both Neogene horsts bounded by major normal faults, and display steep faceted range fronts (figure 2). From west to east, the major normal fault zones in the region are the Wasatch fault zone, West Cache fault zone, and East Cache fault zone (figure 1). This study focuses on the East Cache fault zone.

The East Cache fault zone (ECFZ), at the western margin of the Bear River Range, was first studied by Bailey (1927) and later by Peterson (1936) who first documented Quaternary faulting. Williams (1948) first mapped the fault zone at a scale of 1:125,000, and later at a scale of 1:62,500 (Williams, 1962). Mullens and Izett (1964) portrayed the fault in the Paradise quadrangle at a scale of 1:24,000, but their mapping of the fault was largely derived from Williams (1962). Galloway (1970) included several traces of the fault in her thesis on the Smithfield quadrangle, which was updated by Lowe (1987) and Lowe and Galloway (1993). Cluff and others (1974) performed a photo-geologic analysis of the fault, mapping fault traces at a scale of 1:20,000, but provided no details on geology or the recency or recurrence of faulting. Mendenhall (1975) mapped the ECFZ in the Richmond quadrangle at a scale of 1:12,000. Rogers (1978) mapped geology at a large scale along portions of the ECFZ near Logan and excavated several test pits across suspected faults. Swan and others (1983) performed geologic mapping, scarp profiling, and trenching of the fault between Green Canyon and Providence Canyon. Unfortunately, trenches in that investigation were neither logged nor sampled (D.P. Schwartz, personal communication, 1985). The ECFZ in the Logan quadrangle was most recently mapped by Evans and others (1991).

Interpretation of seismic reflection data by Smith and Bruhn (1984) shows that the ECFZ dips west under Cache Valley at roughly 60° near the surface, flattens to 45° to 55° at depths of 3.5 to 4.0 kilometers (2.1 to 2.4 mi), and probably cuts the Sevier-age Paris thrust (Evans and Oaks, 1990). Net slip on the ECFZ was estimated by Evans (1991) as ranging from a minimum of 2.7 kilometers (1.6 mi) near the Idaho border to a maximum of 8.1 kilometers (4.9 mi) in southern Cache Valley.

The purpose of this study was to more carefully document surface-faulting events in late Pleistocene time and to analyze fault behavior in light of current segmentation models (Schwartz and Sibson, 1989; Hancock and others, 1991). Secondary goals were to compare late Pleistocene fault behavior with longer term Quaternary behavior, and to refine the present estimates for earthquake potential on the East Cache fault zone. Goals were accomplished by four main tasks: (1) surficial geologic mapping along the fault trace, (2) profiling and trenching of fault scarps, (3) deformation analysis of the Bonneville shoreline, and (4) study of the tectonic geomorphology of the Bear River Range front.

SURFICIAL GEOLOGIC MAPPING

Existing surficial geologic mapping along the fault zone (Williams, 1962) could not be used for a modern neotectonic analysis because: (1) at 1:62,500 scale, the mapping was not sufficiently detailed, (2) the base map was not topographic, and (3) surficial units were subdivided according to Lake Bonneville chronologic concepts of the 1950s, now largely revised (see discussion by Scott and others, 1983; Machette and Scott, 1988). Accordingly, surficial geology was remapped during this study along a strip 6 kilometers (3.6 mi) wide, 56 kilometers (33.6 mi) long oriented astride the fault zone in the Paradise, Logan, Smithfield, and Richmond, Utah 7½' quadrangles (McCalpin, 1989).

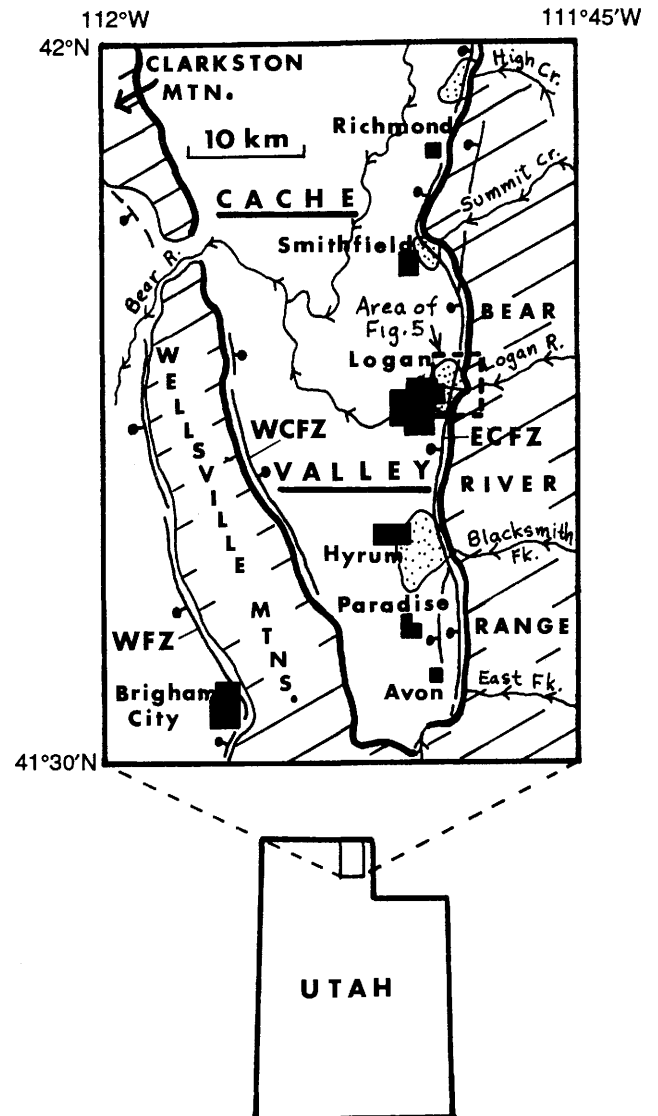


Figure 1. Location map of the study area, showing towns and streams mentioned in text. Dotted areas represent deltas deposited during the occupation of the Provo shoreline of the Bonneville lake cycle. WFZ, Wasatch fault zone; WCFZ, West Cache fault zone; ECFZ, East Cache fault zone.



Figure 2. Oblique aerial photograph of the Bear River Range front on the eastern side of Cache Valley, looking northeast. Providence, Utah is at center; Logan, Utah is at upper left center. The mouths of Logan Canyon and Green Canyon are marked by "L" and "G", respectively. North of Green Canyon the northern section of the ECFZ consists of two splays, marked by dotted lines. South of Green Canyon the central segment of the ECFZ parallels the Bonneville highstand shoreline at the base of a steep, faceted range front. Dashed lines show extent of fault scarps in late Quaternary deposits, whereas the dotted lines indicate the fault position inferred from physiography.

Although the detailed mapping is presented elsewhere (Lowe, 1987; McCalpin, 1989; Brummer and McCalpin, 1990; Evans and others, 1991; Lowe and Galloway, 1993), a general discussion of the stratigraphic framework of Quaternary deposits will familiarize the reader with terminology used throughout this report. Most Quaternary deposits along the ECFZ were deposited during the latest major lake occupation of the Bonneville basin (the Bonneville lake cycle), when Cache Valley was occupied by an arm of Lake Bonneville termed Cache Bay by Gilbert (1890). According to Scott and others (1983) and Currey and Oviatt (1985), deposition during the Bonneville lake cycle began 32 thousand years ago and culminated with the highstand of the Bonneville shoreline (15.5 thousand years ago). Along the ECFZ, the Bonneville highstand shoreline today stands at an elevation of 1,557 to 1,575 meters (5,107-5,165 ft). Failure of the Red Rock Pass threshold about 14 to 15 thousand years ago led to a rapid 100-meter (328 ft) drop of lake level to the Provo shoreline, which was then occupied from 14 to 15 thousand to about 13 thousand years ago. The Provo shoreline along the ECFZ occurs around 1,463 meters (4,800 ft). Lake levels dropped steadily after Provo time, reaching the level of the Great Salt Lake about 11 thousand years ago. Deposits of the Bonneville lake cycle thus include all sediments deposited throughout the lake occupation of Cache Valley (about 30 thousand to 11 thousand years ago), whereas deposits associated with the Bonneville highstand or Provo shorelines were deposited in the narrow time spans cited above. After abandon-

ment of the Bonneville highstand and Provo shorelines, intermittent streams from the smaller mountain canyons deposited alluvial fans at the range front, whereas larger perennial streams cut down through the lacustrine deposits and redeposited shoreline gravels and sands farther valleyward.

QUATERNARY FAULTING AND SEGMENTATION OF THE EAST CACHE FAULT ZONE

The East Cache fault zone forms the boundary between Cache Valley and the Bear River Range for a distance of roughly 80 kilometers (48 mi) from James Peak, Utah, to northeast of Preston, Idaho. In this study only 56 kilometers (33.6 mi) of the fault between 41°30' and 42° N latitude were mapped, where the zone is best expressed topographically. Within that area, the fault is divisible into three physiographic sections based on fault-zone complexity, tectonic geomorphology, and expression of surface fault scarps (figure 3). The descriptive term "sections" is used throughout this report to identify stretches of the ECFZ which are physiographically and structurally distinct, but for which evidence is insufficient to prove that they function as discrete seismogenic rupture segments.

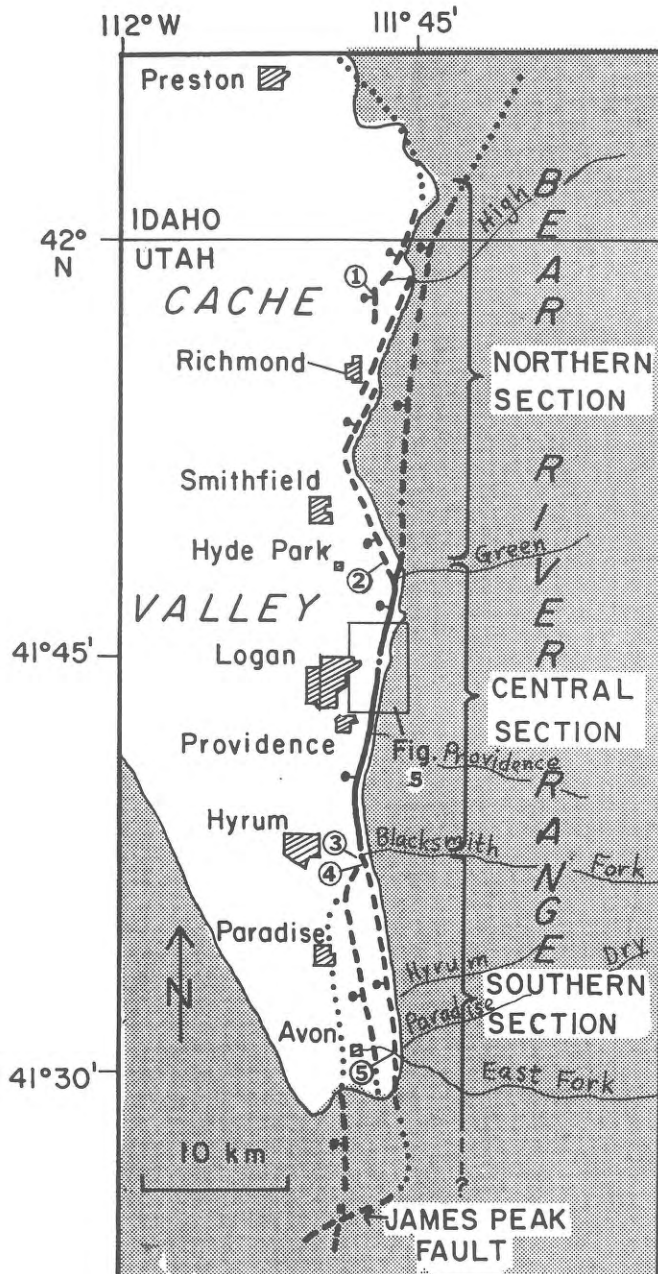


Figure 3. Map of the East Cache fault zone. Fault traces are shown by heavy solid lines where deposits of the Bonneville lake cycle or younger are displaced by surface fault scarps. Dashed lines indicate faulting in late Quaternary deposits, but generally older than 25 thousand years. Dotted lines indicate fault traces inferred from indirect geomorphic evidence such as alignment of drainages and saddles. Circled numbers indicate localities described in text: 1) gravel pit at High Creek, 2) pre-Bonneville pediment offset by 20 meter (66 ft) scarp, 3) water tank cuts, 4) pre-Bonneville fault exposure, 5) canal cuts along the east Fork.

The northern section extends northward from Green Canyon, just northeast of the city of Logan, Utah, at least 26 kilometers (16 mi) to the Idaho border. In this section the ECFZ is characterized by two or three parallel fault traces, by three or four sets of spur facets at the range front and by a lack of fault scarps in

late Pleistocene and younger deposits (McCalpin, 1989). The central section of 16 kilometers (9.6 mi) extends from Green Canyon southward to Blacksmith Fork Canyon (figure 3) and is defined by a single fault trace, a steep range front with seven recognizable facet sets, and fault scarps displacing deltas of the Bonneville lake cycle. The southern section, which is greater than 14 kilometers (8.4 mi) long, extends from Blacksmith Fork Canyon southward to beyond the limits of this study (lat. 41°30' N.), and resembles the northern section because it contains three parallel fault traces, four sets of range-front facets, and fault scarps restricted to middle Pleistocene(?) or older deposits. Nelson and Sullivan (1987, 1992) concluded that the James Peak fault, at the extreme southern end of Cache Valley, is an extension of the southern section of the ECFZ. However, the James Peak fault trends nearly perpendicular to the rest of the ECFZ, and fault scarps cannot be continuously traced between the James Peak fault and the southern section of the ECFZ as defined in this paper (Cluff and others, 1974; McCalpin, 1989). Evidence from fault scarps, faceted spurs, and geophysical studies indicate that the central section of the ECFZ can be considered a seismogenic segment, according to the criteria of Wheeler and Krystinik (1988) and dePolo and others (1991), but its boundaries with adjacent fault sections may be nonpersistent (Wheeler and Krystinik, 1988). In the rest of this report, the terms "central section" and "central segment" are thus used interchangeably.

Westaway and Smith (1989) used range-front physiography to subdivide the entire length of the ECFZ into four "apparent segments" (from south to north 24 kilometers (30 mi), 16 kilometers (9.6 mi), 37 kilometers (22.2 mi), and 16 kilometers (9.6 mi) long). Their central segment is the same as in this report, whereas their two northern segments are either partly or wholly within Idaho (beyond the limits of this study), and their southern section is continuous with the James Peak fault. However, detailed mapping of fault scarps does not support their interpretation of a right-lateral slip component based on a left-stepping enechelon pattern of fault surface (McCalpin, 1989). The combined observations of Westaway and Smith (1989) and McCalpin (1989) indicate that the ECFZ is composed of northern and southern sections of subdued range-front morphology (up to 37 km (22.2 mi) and 24 kilometers (14.4 mi) long, respectively), separated by a 16-kilometer (9.6 mi) section of youthful appearance that is probably a seismogenic segment. In the northern and southern sections, the western trace of the ECFZ separates Quaternary valley fill (to the west) from low foothills of Tertiary bedrock (to the east), while the eastern trace places Tertiary basin fill against lower Paleozoic rocks. In the central section, the ECFZ juxtaposes Quaternary valley fill against lower Paleozoic bedrock with no intervening Tertiary rocks at the surface.

Northern Section

The northern section of the ECFZ consists of two parallel fault strands roughly 2 kilometers (1.2 mi) apart (figure 3). The western strand bounds an irregular and slightly embayed range front developed on the Tertiary Salt Lake Formation (Adamson

and others, 1955), whereas the eastern strand defines a straighter, higher range front developed on lower Paleozoic sedimentary rocks (Williams, 1948, 1962). Several bedrock outliers are present between these two range fronts (Richmond Knoll, Crow Mountain, Long and Round Hills); these may be composed in part of mega-landslide blocks derived from the eastern range front during late Tertiary time (Brummer, 1990; Brummer and McCalpin, 1990).

No geomorphic surfaces of the Bonneville lake cycle or younger age are displaced by the western fault strand. The only Pleistocene fault scarp in this section occurs at the extreme southern end of the western fault strand, about 3 kilometers (1.8 mi) north of the boundary with the central section. Here a pre-Bonneville pediment surface is apparently displaced across the fault trace about 20 meters (65.6 ft) vertically (figure 3, location 2). The fault trace is marked by a broad, subdued ramp, indicating significant time has passed since latest faulting.

A gravel pit near High Creek on the western fault strand of the northern section (figure 3, location 1) reveals a complex 30-meter-wide (98 ft) fault zone in Provo-level delta deposits (figure 4). Several faults are truncated by channels (units 4, 5, and 6, figure 4) near the delta surface; these channels are restricted to the structural depression formed by a graben. The faults have no surface expression north or south of the gravel pit, despite the fact that the gently sloping Provo delta surface is well preserved over a distance of 2 kilometers (1.2 mi) to the south (McCalpin, 1989). These relationships suggest that these structures formed late during the deposition of the Provo delta, while the delta surface was still active. After faulting, the active delta channels were diverted into the graben where they deposited several channel fills. Late Provo topset beds (unit 7, figure 4) subsequently covered the entire deposit. No numerical ages were obtained from this short-lived exposure, but Provo deposits

have been dated elsewhere between 12.8 and 13.4 thousand years ago (Currey and Oviatt, 1985).

Apparent faulting in the High Creek gravel pit exposure, and in a similar pit 1 kilometer (0.6 mi) south, raises several questions: (1) if surface faulting occurred at these locations about 13 thousand years ago, why are no fault scarps observed in other Bonneville-lake-cycle deposits along the range front, (2) why is faulting found only near the front of Provo-level deltas, roughly 1 kilometer (0.6 mi) valleyward of the range-front escarpment, and (3) is the similarity of inferred fault timing on the northern section (13 thousand years ago) and on the central section (12.8 to 15.5 thousand years ago; see next section) coincidental. All three questions can be answered satisfactorily if the High Creek structures represent lateral spreading of the delta front during seismic shaking, and not surface rupture on the northern section of the ECFZ. Seismic shaking from a faulting event on the central section could easily have produced lateral spreading in an active Lake Bonneville delta which lies only 20 kilometers (12 mi) north of the central section. However, other ground deformation features such as sand blows or contorted lacustrine strata have not been observed in the northern section of the ECFZ, although they are abundant in the central section.

A north-trending, down-to-the-east normal fault not associated with a delta front is exposed in a road cut in the NW¼ section 12, T. 12 N., R. 1 E. about 1 kilometer (0.6 mi) east of Hyde Park, but this fault displaces only pre-Bonneville alluvium by 1.5 meters (4.9 ft) (Lowe, 1987). No evidence of displacement is seen at the ground surface, which is composed of lake bottom sands of the Bonneville lake cycle. Because evidence for true tectonic faulting in Bonneville-age and younger deposits is equivocal in this section of the ECFZ, latest faulting is presumably older than 15 thousand years ago.

On a longer time scale, movement on the western strand of

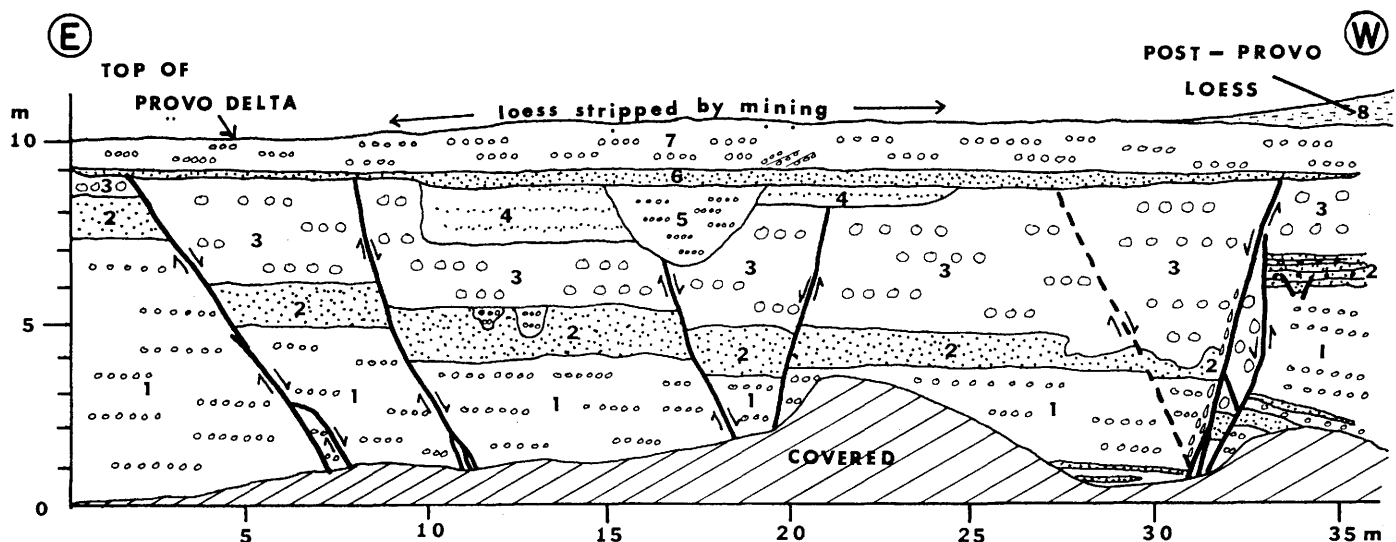


Figure 4. Sketch of multiple faults in a gravel pit wall in a Provo-level delta at the mouth of High Creek (location 1 in figure 3). Lithologic symbols: dots and dashes, silt; dots, sand; small circles, pebble gravel; large circles, cobble gravel. The faults define a broad graben with net throw down-to-the-west of about 1 meter (3.3 ft). These faults do not displace the ground surface, and may represent lateral spreading toward the delta front (off of sketch to the right) during earthquake shaking. Unit numbers are for descriptive purposes only, and correlate with the brief discussion in the text.

the ECFZ has truncated Neogene pediments cut onto the Salt Lake Formation between Hyde Park and Richmond (figure 3). These pediments are only offset 20 meters (65.6 ft) at the southern boundary of the section (figure 3, location 2), but pediment remnants gradually rise to elevations of 500 meters (1,640 ft) above the base of the valley floor near Richmond, Utah. These pediments must have extended west of the ECFZ when formed, but are now covered by Quaternary sediments on the western (downthrown) side of the ECFZ; net Neogene slip across the ECFZ on the western strand must therefore be at least 500 meters (1,640 ft). In contrast, the Franklin Ramp, (a large pre-Bonneville pediment surface east of Franklin, Idaho, 1 kilometer (0.6 mi) north of the study area) crosses the ECFZ without being displaced. Although the age of the Ramp is unknown, the Bonneville highstand shoreline is visible across it, as are patterned gravel phenomena, so it almost surely predates the Bonneville lake cycle and latest glaciation (35-15 thousand years ago). If the Ramp is middle Pleistocene in age and is unfaulted, then truncated pediments cut on the Miocene and Pliocene (?) Salt Lake Formation between Hyde Park and Richmond must be at least early Pleistocene in age.

On the eastern fault strand, Tertiary bedrock may be in fault contact with Paleozoic rocks for the southernmost 5 kilometers (3 mi) of this section, but to the north the contact has been variously interpreted as a steep (24-45 degrees) unconformity (Galloway, 1970; Mendenhall, 1975) or as a low-angle normal fault (Brummer, 1990; Brummer and McCalpin, 1990). Neogene displacement is inferred to occur within the Tertiary rocks south of Cherry Creek, whereas to the north the fault juxtaposes Salt Lake Formation against unnamed Precambrian quartzites (Mendenhall, 1975).

Near the southern boundary of the northern section, most displacement must be taken up by the eastern splay, as indicated by a steep range front in Paleozoic rocks and by very low pediment offsets on the western splay. As the fault is traced northward, pediment offsets on the western splay increase rapidly to over 200 meters (656 ft), while the range front of the eastern splay becomes morphologically subdued. North of Hyde Park Canyon, the eastern splay may pass into an unconformity (?) and pediment offsets on the western splay stabilize at 400 to 500 meters (1,312-1,640 ft). This geometry suggests a progressive northward shift of late Cenozoic displacement from the eastern to the western splay. Westaway and Smith (1989) map the eastern splay fault as defining a range front with declining relief that extends another 11 kilometers (6.6 mi) north into Idaho. If this range front is also part of the northern section of the ECFZ, then its total length would be 37 kilometers (22.2 mi).

Slip Rate And Recurrence

With the scarcity of offset late Quaternary deposits in this section, very little can be said about the slip history and probability of future displacements. The location of the fault trace is uncertain because of the antiquity of the faulting and the coincidence of the Bonneville shoreline with the western splay of the ECFZ along the northern half of the section. The alignment of graben structures in two gravel pits in Provo deltaic sediments may indicate a "hidden" splay of the ECFZ, but it is more likely

that the two sites failed by shaking-induced slumping of delta fronts.

Assuming an early Pleistocene age (about 1-2 million years) for the faulted pediments (Williams, 1948), the long-term slip rate would be 0.25-0.5 mm/yr (0.01-0.02 in/yr). At that rate, slip since the occupation of the Bonneville shoreline (15 thousand years ago) should amount to 3.8 to 7.5 meters (12.5-24.6 ft), yet no displacement is observed in Bonneville or younger deposits. The discrepancy indicates that the long-term slip rate may be an overestimate, or more likely, that slip rate is variable through time.

Central Section

The central section of the ECFZ extends from Green Canyon south to Blacksmith Fork Canyon (figure 3), and is typified by a single, straight fault trace located at the base of a rugged range front cut into upper Proterozoic and Paleozoic rocks (figure 2). Fault scarps displacing Bonneville-lake-cycle or younger deposits occur on the northern half of this section, where scarps diverge as much as 400 meters (1,312 ft) westward from the base of faceted spurs between Green Canyon and Providence Canyon (figure 5). South of Providence Canyon, post-Bonneville faulting may have occurred, but no scarps are preserved; mass movements at the base of faceted spurs may have obliterated evidence of young faulting.

Swan and others (1983) mapped fault scarps between Green and Providence Canyons and measured three scarp profiles with net tectonic offsets of 1.4 meters (4.6 ft), 2.75 meters (9.0 ft), and 1.5 to 1.8 meters (4.9-5.9 ft). Between Green and Logan Canyons, scarps offset Bonneville-highstand-shoreline sands and silts, the Provo delta, and a post-Provo strath terrace roughly 12 meters (39.4 ft) below the Provo delta surface (at the "Provo" trench, figure 5). A "test pit" across a scarp 150 meters (492 ft) south of Green Canyon (marked "WC" on figure 5) exposed a "20-m (65.6 ft) wide zone containing 6 to 7 faults having down-to-the-west displacement" (Swan and others, 1983, p. 6). No displacement data from the trench were given in that report; because the scarp traverses irregular transgressive shoreline topography, net offset at their trench site could not be reconstructed by surface profiling. However, multiple events were inferred by Swan and others (1983, p. 6) based on observed faulting of scarp-derived colluvium.

Multiple west-facing escarpments between the Bonneville and Provo shorelines may be fault scarps (as implied by mapping of Cluff and others, 1974) or transgressive shorelines. A trench excavated for a City of Logan water line in July, 1987, 1.7 kilometers (1.0 mi) south of Green Canyon, across a subdued 5-meter-high (16.4 ft) scarp east of the mapped trace of the ECFZ, was observed by the author to contain a greater than 2 meter (>6.6 ft) down-to-the-west displacement of Bonneville transgressive gravels and overlying loess. This evidence suggests that at least some of the scarps mapped by Cluff and others (1974) between the Bonneville highstand and Provo shorelines may be underlain by faults in the area between Green and Logan Canyons.

The scarps of 1.2 to 3.0 meters (3.9 - 9.8 ft) on the Provo delta mapped by Swan and others (1983, figure 7) represent 1.4 meters (4.6 ft) of net vertical tectonic displacement, spread over a broad graben zone up to 100 meters (328 ft) wide. The underlying fault was exposed in the 1930s in a vertical south-facing road cut of U.S. Highway 89 near the center of the post-Provo terrace (figure 5). The vertical face is no longer exposed due to degradation of the road cut and burial by colluvium. Peterson (1936) shows a photograph (figure 6) of well-laminated Bonneville-lake-cycle sands and silts (prodelta?) overlain by about 3.4 meters (11.1 ft) of bouldery strath terrace gravel. The contact between the sandy prodelta deposits and underlying (transgressive?) gravels is displaced along a vertical fault by 6.4 to 6.8 meters (21.0-22.3 ft), while the base of the strath terrace gravels appear to be displaced an amount similar to the surface scarp height (1.3 m; 4.3 ft). This geometry argues for recurrent faulting, with perhaps two to four events offsetting the prodelta deposits, the latest of which also offset the overlying strath terrace and Provo delta surface. Late Holocene alluvial fans north of Logan Canyon are not faulted, and one fan immediately north of the Logan Country Club golf course (figure 5) clearly buries the scarp that displaces the Provo delta, indicating no late Holocene faulting.

South of Logan Canyon, the fault ascends a steep gully and then is well-expressed across the surface of the Bonneville highstand delta as a west-facing fault scarp (figure 5). Between Logan Canyon and Dry Canyon the scarp is about 150 meters (492 ft) west of the range front, but converges with the front to the south and loses expression 2 kilometers (1.2 mi) south of Logan Canyon. Vertical surface offsets in Bonneville highstand shoreline deposits, reconstructed from eight scarp profiles in this 2 kilometer (1.2 mi) stretch, range from 2.2 to 4.2 meters (7.2-13.8 ft) (figure 5 and table 1). The scarps are best expressed on the tops of ridges of dissected Bonneville-highstand nearshore sands and silts, and do not offset Holocene alluvium in gullies between the ridges. Swan and others (1983, p. 7) noted that "the fault scarp ... is visible on the steep sides of the gullies, indicating that at least some of the faulting that produced the scarp occurred after the Bonneville deltaic deposits were eroded." Other evidence for the multiple-event nature of this scarp includes: (1) the surface offsets (2.2-4.2 m; 7.2-13.8 ft) are roughly twice that of the scarps that displace younger (Provo and post-Provo) deposits north of Logan Canyon (figure 5), and (2) inflections are present in some scarp profiles (Swan and others, 1983, figure 7, profile B). A trench excavated across the main fault scarp south of Logan Canyon (the Bonneville trench on figure 5) uncovered stratigraphic evidence for two post-Bonneville-highstand faulting events (see next section).

Head scarps of old landslides are also common in Bonneville sands and silts along the 2 kilometer (1.2 mi) stretch between Logan Canyon and Dry Canyon (figure 5; see also Swan and others, 1983, p. 7). All landslide scarps are truncated by gullies which dissect the Bonneville sediments. Furthermore, no landslide deposits are preserved below the scarps on Provo deltas or on alluvial fans graded to the Provo delta. These geomorphic relations indicate that the landslides occurred before or during the occupation of the Provo shoreline. Wave and stream action on the delta surface obliterated landslide deposits, after which gullies graded to the Provo shoreline were cut into the landslide

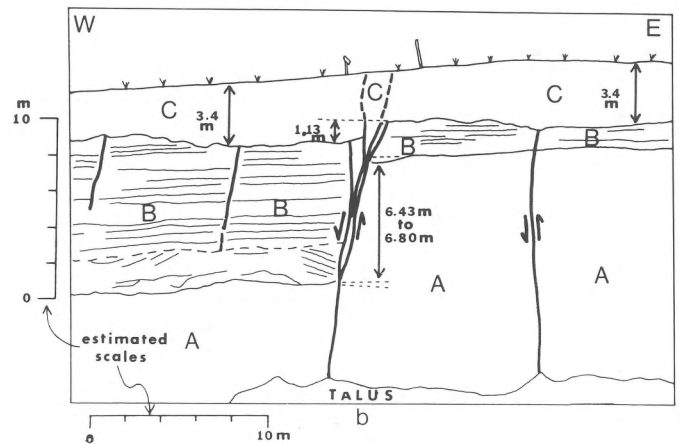
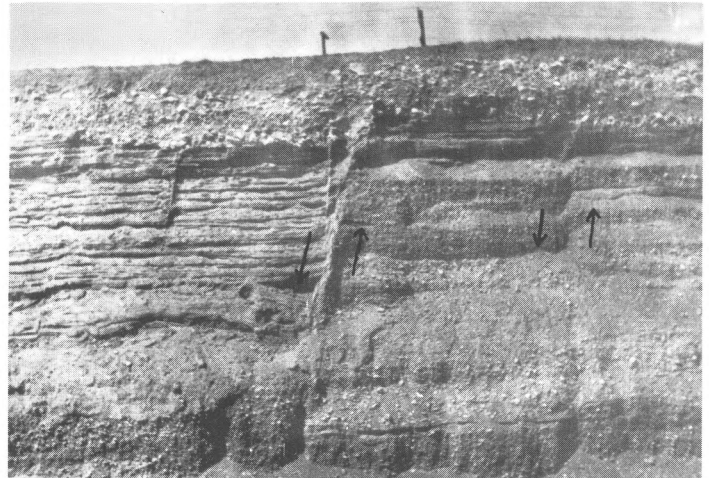


Figure 6. Photograph and sketch of U.S. Highway 89 roadcut at the mouth of Logan Canyon. A) photograph of the roadcut taken in the 1930s, from Peterson (1936). B) Author's annotation of the Peterson photograph, showing correlation of strata and inferred displacement on faults. The photograph was scaled assuming the thickness of the post-Provo strath terrace gravels (unit C) was 3.4 meters (11 ft), as measured on the opposite side of US 89. No correction was made for perspective distortion on the photograph, so vertical scale varies. Unit B=Bonneville prodelta sands and silts (?); unit A=well-stratified gravels, possibly related to the Bonneville transgression. The trench in figure 11 was located on the strath terrace surface directly above the main fault in the center of the photograph.

terrain. Evidence from the trench on the Bonneville delta indicates that these landslides may have been slumps triggered by surface faulting soon after the Bonneville flood (see trench discussion below).

Between Hell's Kitchen (figure 5) and Providence Canyon (figure 3) the range front is dominated by Holocene alluvial fans that do not display fault scarps. Several north-trending lineaments in lake deposits north of Providence Canyon may be tectonic or transgressive shorelines. However, a single, large, anomalous scarp exists 700 meters (0.4 mi) north of Providence



Figure 7. Photograph of the trace of the ECFZ on the Bonneville delta surface south of Logan Canyon, immediately north of the Bonneville trench. The west-facing, 6-7-meter-high (22 ft) scarp at right center is the location of scarp profile no. 1 (table 1). Vehicle tracks at center occupy a back-tilted area 50 meters (164 ft) wide at the base of the fault scarp.

Canyon at roughly the level of the Bonneville shoreline. The scarp is developed in an eroded remnant of pre-Bonneville fan alluvium and has a minimum height of 21 meters (69 ft) and surface offset of 8.5 meters (27.9 ft) (table 1, profile 9). Surface offset is a minimum because the scarp base is buried by Bonneville-highstand shoreline deposits. This scarp has been partly created by shoreline erosion at the Bonneville level, but must be at least partly tectonic because the Bonneville highstand shoreline is extremely indistinct both north and south of this old fan remnant. This location is the only one in the central section where pre-Bonneville deposits have surface expression of faulting.

Immediately south of Providence Canyon a 3.75-meter-high (12.3 ft) northwest-trending scarp offsets a gravelly Bonneville-highstand delta. This short scarp has a very anomalous strike, and does not seem to align with known scarps north of Providence Canyon, although it does parallel an abrupt direction change in Spring Creek to the west. Because an erosional origin is not indicated, it has been assumed that the scarp is tectonic (Swan and others, 1983, p. 8). The net surface offset across the scarp is estimated as 1.5 to 1.75 meters (4.9-5.7 ft), but estimates are difficult because of the width (70-80 m; 230-262 ft) of the back-tilted zone west of the scarp.

From Providence Canyon to Blacksmith Fork Canyon, the range front forms a broad west-facing arc, along which no fault scarps are visible. If post-Bonneville surface faulting extended into the southern half of the central section, any scarps produced have been buried by Holocene fans or destroyed by rapid range-front erosion.

The Bonneville Trench

The ECFZ was exposed by a backhoe trench 65 meters (213 ft) long and 2.5 to 3.5 meters (8.2-11.5 ft) deep, herein referred to as the Bonneville trench, across the Bonneville-highstand

delta 0.9 kilometers (0.5 mi) south of Logan Canyon. The trench is located from 80 to 140 meters (262-460 ft) west of the Bonneville highstand shoreline (figure 7) at an elevation of 1,557 to 1,564 meters (5,107-5,130 ft), or 3 to 10 meters (9.8-32.8 ft) below the elevation of the Bonneville shoreline. The 45 units logged in the trench (appendix 1) fall into seven lithostratigraphic packages (figure 8). Packages 1, 2 and 3 (units 1-39) are nearshore laminated sands and imbricated gravels of the Bonneville highstand level of Bonneville lake cycle. Package 4 is a heterogeneous mixture of intact blocks and disaggregated material derived from packages 1, 2, and 3 that is inferred to have slid and rolled down a fault scarp free face. Package 5 may be the distal facies of package 4 (debris flow?). Package 6 consists of loess-rich colluvium that buried the initial fault scarp and was later offset by a second faulting event. Package 7 is colluvium and slopewash that postdates the second faulting event.

Tectonic features in the trench include the main fault trace under the central, steepest part of the scarp profile (figure 9), subsidiary small-displacement shears in the upthrown block (all within 4 meters [13 ft] of the main trace), and a single antithetic fault (0.8 meters; 2.6 ft stratigraphic displacement) 27 meters (88.6 ft) west of the main trace. Due to the unknown initial dip component of cross-bedded gravels within the graben, it is difficult to say whether back tilting has been significant. Notably, we observed no tectonic features of any kind in the interior of the graben.

Net surface offset is 2.6 meters (8.5 ft) across the main scarp and 2.4 meters (7.9 ft) across the entire 35-meter-wide (115 ft) deformation zone. Displacement occurs on six major faults (lettered A through F on figure 8b) that dip westward at 65 to 75 degrees near the trench floor and steepen to nearly vertical near the surface. The total vertical stratigraphic displacement of 4.3 meters (14.1 ft) is measured by projecting the top of lacustrine gravels (units 4-11) upslope of the scarp, downslope over the faulted gravels of the downthrown block (unit 16). Several small antithetic faults dip eastward at 55 to 75 degrees and have vertical displacements of up to 10 centimeters (3.9 in). Massive sand from unit 1 was evidently mobilized upwards along faults A and B to form features resembling sand blows (figure 8b). The 80-centimeter-wide (2.6 ft) zone between the upper parts of faults E and F is filled with displaced blocks of silt and sand in a matrix of deformed sand, and may represent a tension crack fill.

Cross-cutting relationships, and the difference between displacements of a distinct, fine-sand marker bed in unit 1 (marked "m" on figure 8b) versus displacements of the major unconformity (heavy wavy line, figure 8b) allow offsets on some of the six major faults to be partitioned between the earlier and later faulting events. The method for differentiating these displacements is as follows (from McCaLpin and Forman, 1991). Total vertical displacement from both faulting events was measured based on offset of the fine-sand marker bed in unit 1, whereas displacement during the later event was measured from offsets of the major unconformity underlying the debris from the first-event free face (units 40, 41, and 42). Displacement inferred for the earlier event is the difference between total displacement and displacement due to the later event. Below

Table 1. Fault scarp profile data, East Cache fault zone.

Location ¹	Profile #	Surface slope(°) ³	Maximum scarp slope angle(°)	Scarp height(m) ⁴	Surface Offset(m) ⁵	Faulted Deposit
between Logan Canyon and Hell's Kitchen (from north to south)	1	3	10	6.7	2.5	Bonneville delta
	2	3	14	6.3	2.5	Bonneville delta
	3	3	11	6.0	3.3	Bonneville delta
	4	6	16	6.1	4.2	Bonneville beach sands
	5	6	23	6.4	2.2	Bonneville beach sands
	6	9	17	3.9	0.4	Bonneville beach sands
	7	6(?)	21	4.1	0.9	Bonneville beach sands
N. of Logan Canyon	A ²	-	-	3.0	1.4	Provo delta
S. of Logan Canyon	B ²	-	-	-	2.8	Bonneville delta
S. of Providence Canyon	8	0	13	3.2	2.8	Bonneville delta
same as above	C ²	-	-	-	1.5-1.75	Bonneville delta
N. of Providence Canyon	9	10	33	19.3	>8.5	pre-Bonneville fan
N. of Paradise Dry Cyn.	10	9	24	15.8	10.0	pre-Bonneville fan
between Hyrum and Paradise Dry Cyn.	12	12	21	20.3	1.4	pre-Bonneville pediment
	13	10-12	22	31.5	1.2-5.5	pre-Bonneville pediment

¹ also located on figure 4

² letters refer to scarp profiles from Swan and others, 1983, figure 7; only surface offset data were given.

³ gradient of the faulted geomorphic surface

⁴ graphically measured by the method of Bucknam and Anderson, 1979

⁵ graphically measured as the vertical distance between projected offset surfaces.

the faults on figure 8b, numbers before and after the slash are vertical displacements (in centimeters) during the earlier and later faulting events, respectively; T is the total vertical displacement (in centimeters).

Twenty-seven meters (88.6 ft) downslope from the main fault zone a narrow antithetic fault zone exhibits 0.8 meters (2.6 ft) of vertical stratigraphic displacement in package 3, but only creates a weak inflection of the ground surface (figure 8a). The fault zone apparently displaces the base of unit 43 by about 40 centimeters (1.3 ft), indicating that about half of its total displacement occurred during each of the two faulting events.

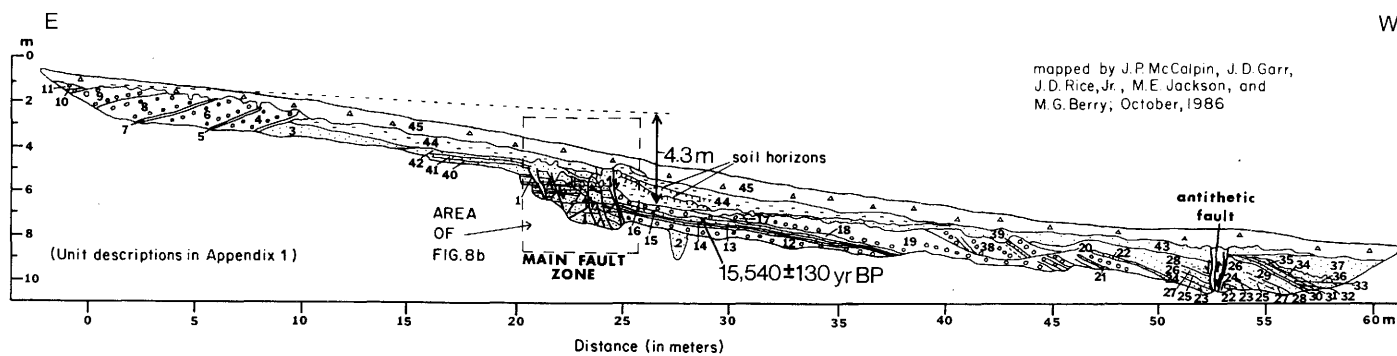
Numerical ages: Only a single sample suitable for radiocarbon dating was retrieved from the trench. Gastropod shells from unit 15 yielded an accelerator mass spectrometry radiocarbon age of $15,540 \pm 130$ yr B.P. (AA-4017). This age correlates well with other radiocarbon ages from Bonneville highstand deposits, which range from 15.4 to 16.1 thousand years (Currey and Oviatt, 1985, table 1), and it provides a maximum limiting age for the earlier of the two faulting events.

The presence of fine, sandy, lacustrine deposits and loess-rich colluvium in the trench indicated that thermoluminescence (TL) dating might be useful in dating the inorganic units. Previous work has shown that shallow marine sands (Forman and others, 1987; Forman, 1989) and loess (Wintle and Huntley, 1982; Rendell and Townsend, 1988) both yielded accurate TL age estimates, so six TL samples were collected from the Bonneville trench (figure 8b). Laboratory procedures and criteria for acceptable counting statistics are given in McCalpin and Forman (1991). All TL analyses were performed by Alpha Analytic Inc. of Coral Gables, Florida.

Chronology of faulting: Two post-Bonneville-highstand faulting events are recognized in the Bonneville trench. We hereby summarize evidence that constrains the timing of each event, based on: (1) stratigraphic relations, (2) radiocarbon and TL age estimates, and (3) geomorphic relations between fault scarps and Quaternary deposits in the central section.

The log of the Bonneville trench (figure 8a) shows that the lacustrine sands and gravels have been faulted about 4.3 meters (14.1 ft) down to the west during the earlier event. I infer that prior to faulting, the trench site was occupied by a north-trending littoral bar, cored with horizontally bedded sand (units 1 and 2) and veneered with a "shell" of gravel with opposing cross-bed directions (units 3-39). The earlier faulting event produced a cumulative stratigraphic displacement of 3.1 meters (10.1 ft) on faults D, E, and F (figure 8b and table 2) and displaced the bar near its center, exposing the sand core in the free face. The exposed sand core presumably failed rapidly in an avalanche of loose sand and sand blocks to form units 40-42 and their basal unconformity. This heterogeneous mixture of sand and sand blocks, plus the presence of features like sand blows, initially indicated that faulting had occurred under water (McCalpin, 1987a, 1988). Geomorphic relations (described later) show that lake level had abandoned this surface by the time of faulting, so liquefaction features may have resulted from a local high water table. Unit 43, present only on the downthrown block, was probably derived from the gravel which covered the bar crest, which slid downslope as a thin debris flow during or after the faulting event (figure 8a). Following deposition of units 40 through 43, the scarp profile declined due to subaerial erosion, and unit 44 (the silty colluvium) was deposited against and across

mapped by J.P. McCalpin, J.D. Garr,
J.D. Rice, Jr., M.E. Jackson, and
M.G. Berry, October, 1986



		EXPLANATION						
PACKAGE	→	1	2	3	4	5	6	7
UNITS	→	1-2	3-11	12-39	40-42	43	44	45
LITHOLOGY	→	med. sand	gravel	gravel + sand	sand	diamicton	silt	sd. gravel
ORIGIN	→	shorezone	beach	beach	shorezone	debris flow	colluvium	slopewash
AGE	→	← Bonneville highstand →				latest Pleistocene	early Holocene	mid-late Holocene

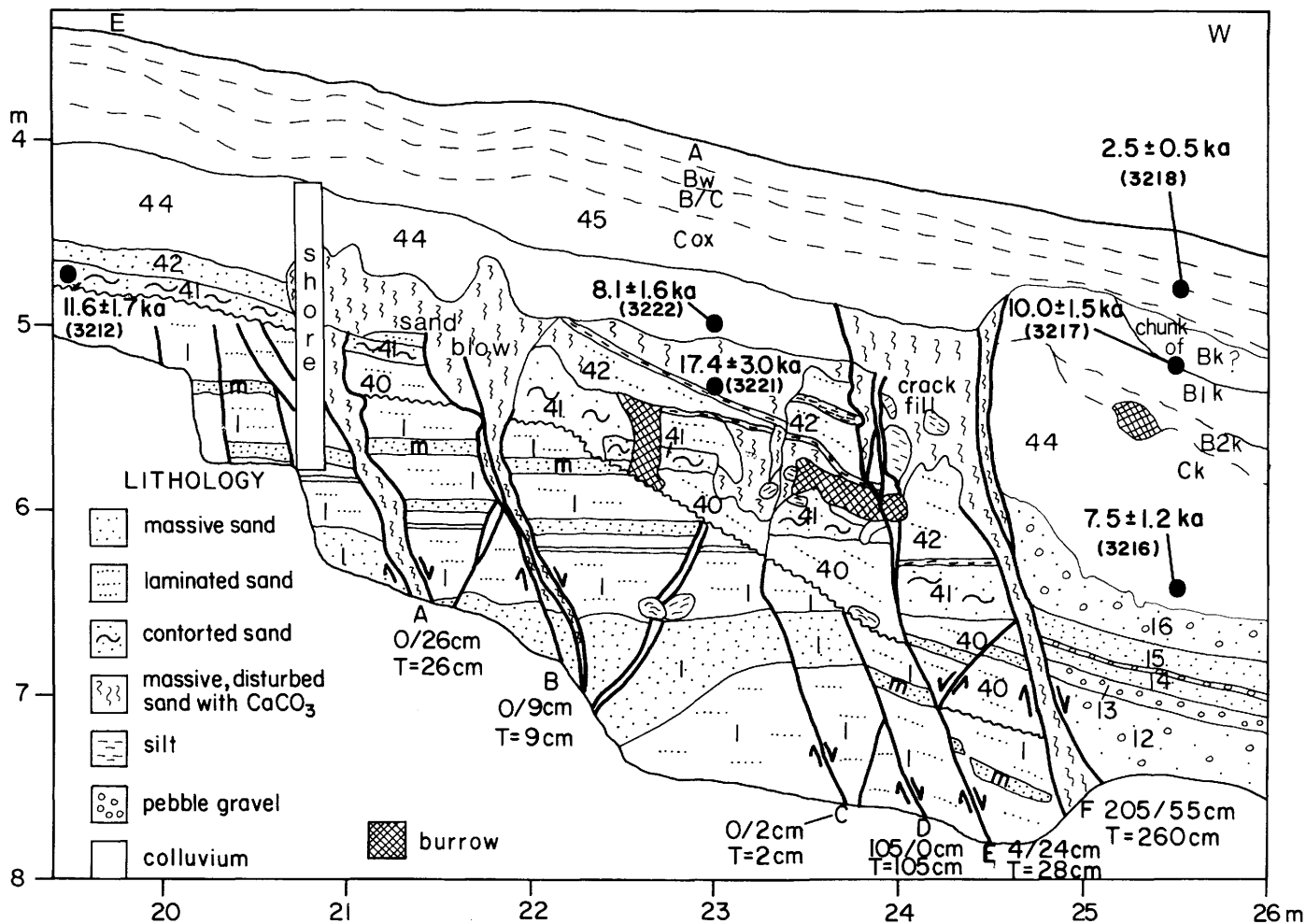


Figure 8. Log of the Bonneville trench across the central section of the ECFZ. (A) Simplified log of the entire trench. Numbers refer to descriptions in appendix 1. Total stratigraphic displacement at the main fault, based on projection of the top of lacustrine beds on the upthrown block, is 4.3 meters (14.1 ft). Radiocarbon age of $15,540 \pm 130$ yr B.P. is from gastropod shells in unit 15. (B) Detailed log of the main fault zone. Black circles indicate TL sample locations (to scale). Numbers under lettered faults (A-F) indicate vertical displacement in the earlier and later faulting events, respectively; T = total displacement (see table 2). Unit numbers correspond to figure 8 and appendix 1. Bed "m" is a distinct sandy marker bed used to calculate cumulative fault displacements. Soil horizon nomenclature is explained in the text.

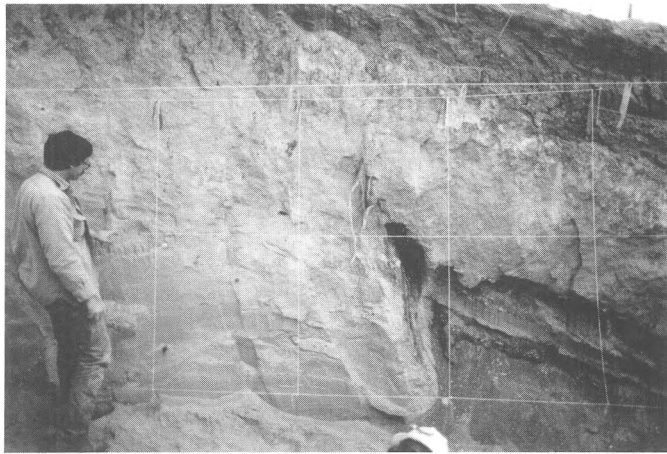


Figure 9. Photograph of the main fault zone in the Bonneville trench. String lines define a 1-meter (3.3-ft) grid; vertical lines correspond to horizontal distance markers 23 meters (75.4 ft) (on left) through 26 meters (85.3 ft) (on right) on the bottom scale of figure 8b. Fault F at right center accounts for most of the total stratigraphic displacement, and juxtaposes Bonneville high-stand gravels (at lower right) against Bonneville littoral sands.

the scarp. Thus the earlier faulting event postdates units 1-39, is contemporaneous with units 40-42 (and possibly unit 43), and predates unit 44.

Two TL age estimates on units 41 and 42 that should be contemporaneous with faulting are somewhat contradictory. Sample 3221 from the lateral equivalent of the sand blow from fault B (figure 8b) yielded a TL age estimate of 17.4 ± 3.0 ka. This date is older than that of stratigraphically lower unit 15 and appears to be erroneously old. The geometry shown in figure 8b suggests that the sand was ejected onto the surface of unit 42 from a source bed within unit 1, probably near the base of fault B. Eyewitness accounts of sand-extrusion in historic earthquakes (Fuller, 1912) indicate that sand-blow deposition is very rapid, so a majority of sand grains probably would not receive sufficient (8 hours) new sunlight exposure to "re-zero" the TL signal. As a result, the TL age estimate for sample 3221 may more closely date the initial deposition of the lacustrine sand (in a stratigraphically lower position somewhere within unit 1) than its redeposition during faulting. Sample 3212 was collected near the upslope flank of the sand blow (unit 41) where weakly contorted but finely laminated medium to fine sand was quite distinct from the massive sand associated with the sand blows (figure 8b). The TL age estimate of 11.6 ± 1.7 ka (sample 3212) is reasonable compared to the age of underlying unit 15 ($15,540 \pm 130$ yr B.P.; AA-4017) and overlying unit 44 (7.5 ± 2 ka, sample 3216 to 10.0 ± 1.5 ka, sample 3217). Finally, three TL age estimates on the post-earlier event colluvium (unit 44) provide minimum ages on faulting. Samples 3216 and 3222 from near the base of unit 44 on the downthrown and upthrown

Table 2.
Vertical displacements on individual faults and across entire deformation zone, Bonneville trench.

SYNTHETIC FAULTS	VERTICAL DISPLACEMENT (cm)		
	Total	In Earlier Event	In Later Event
A	26	0	26
B	9	0	9
C	2	0	2
D	105	105	0
E	28	4	24
F	260	205?	55? ¹
SYNTHETIC TOTAL	430	314	116
ANTITHETIC FAULT	-80	-40? ²	-40?
BACKTILTING ³	-95	-95	0
NET ACROSS ENTIRE ZONE	255	179	76

¹Questionable value, measured as vertical difference between the base of unit 6 on either side of the tension crack fill between faults E and F. If the base of unit 6 had an original valleyward gradient (probable), then 55 centimeters (1.6 ft) is a maximum value.

²Estimated value, assuming half of total displacement occurred in each event. The ground surface and unit 5 are weakly warped over the fault, suggesting minor displacement during the second event.

³Back tilting of the downthrown block of roughly 4° (based on divergence of unit 513b contact from the ambient faulted surface) over a horizontal distance of 13.5 meters (44 ft) (see figure 4) results in 95 centimeters (3.1 ft) of tilt-induced slip on fault F. Because the top of unit 6 has a similar gradient to that of the modern ground surface it is assumed to be untilted, and thus all tilt is assigned to the earlier faulting event.

blocks, respectively, yield similar estimates of 7.5 ± 1.2 ka (3216) and 8.1 ± 1.6 ka (3222) (figure 8b); however sample 3222 exhibited greater than 10 percent fading and may be somewhat older. The 10.0 ± 1.5 ka age estimate for sample 3217 gives a weak apparent chronologic reversal, which is not significant at 1 sigma error limits. Sample 3217 was from a block of soil horizon which I infer fell from the second-event free face, hence its original stratigraphic position is unknown. In light of the age spread of these dates, we assign the mean (including a 10 percent increase for fading in samples 3217 and 3222) of 8.7 ± 1.0 ka as the age of the basal part of unit 44.

Stratigraphic and numerical-age data from the Bonneville trench thus bracket the earlier faulting event between a mean TL age estimate of 8.7 ± 1.0 ka and a radiocarbon age of $15,540 \pm 130$ yr B.P., with the suggestion that a deposit dated at 11.6 ± 1.7 ka is contemporaneous with faulting. An additional age constraint is imposed by the observation of Swan and others (1983) that fault-scarp heights are twice as large on the Bonneville-highstand delta than on the Provo-level delta (figure 5). This

geometry implies that the earlier faulting event expressed on the Bonneville-highstand delta predated the formation of the Provo delta surface. Currey and Oviatt (1985) bracket the occupation of the Provo shoreline between about 12.8 and 13.4 thousand years ago. This additional geomorphic constraint indicates that the earlier faulting event on the central section must have occurred between about 12.8 to 13.4 thousand years ago and $15,540 \pm 130$ yr B.P. The TL age estimate from unit 41 (sample 3212, 11.6 ± 1.7 ka) which barely overlaps the youngest part of this age range at one sigma, is considered a less reliable constraint on age of faulting because its stratigraphic relation to faulting is not clear.

The later faulting event also left traces in the trench. The early loess-rich colluvium in the Bonneville trench (unit 44) has subsequently been displaced along faults E and F, and the unconformity at the base of units 40-42 was displaced by faults A, B, and C (figure 8b and table 2). The sand blow-like features emanating from faults A and B are associated with a 35 centimeter (1.1 ft) vertical displacement of the unconformity. In the fault B sand blow a discrete fault plane can be traced upwards into the sand blow material and the upper contact of overlying unit 44 package 6 is warped by 9 centimeters (3.5 in), indicating that most (if not all) of the 9 centimeters (3.5 in) of stratigraphic displacement on fault B must have occurred during the later faulting event. By noting differential vertical displacements between the fine-sand marker bed in unit 1 and the unconformity at the base of unit 4, displacements can be partitioned between the earlier and later faulting events (table 2).

Prior to the later faulting event a strong soil developed on unit 44. This soil (horizons B1k, B2k, Ck; figure 8b) is now only preserved on the downthrown block; the soil on the upthrown block was eroded following the second faulting event. A displaced piece of Bk horizon (contains TL sample 3217, figure 8b) appears to be a block of soil that fell to the base of the free face following the later faulting event. No discrete wedge of colluvium from the later faulting event was exposed in the trench. Instead, it appears that much of the earliest derived colluvium from the second-event free face fell into a tension crack between faults E and F. Later colluvium is spread as a relatively uniform layer over the entire scarp face (unit 45). This lack of a wedge-shaped colluvial deposit is often associated with multiple, small-displacement faulting (≤ 1 m; ≤ 3.3 ft) on a pre-existing slope (Ostenaar, 1984; McCalpin, 1987b). A moderately developed soil with a cambic B horizon is formed on the youngest slope colluvium (unit 45), so this deposit may be several thousand years old (Shroba, 1980).

The mean of TL age estimates for the basal part of the earlier colluvial wedge (8.7 ± 1.0 ka) provides only a maximum limiting age for the later faulting event. The lower part of unfaulted unit 45 yielded a TL age estimate of 2.5 ± 0.5 ka (sample 3218, figure 8b). Sample 3218 postdates faulting by the time needed to degrade the free face created by faults E and F, and to deposit the lower half of unit 45. The time window of 2.5 to 8.7 thousand years is too large to tightly constrain faulting, so geomorphic evidence has been used to decrease this interval.

Holocene alluvial fans along the ECFZ are not faulted, so their age could provide another minimum limiting date on faulting. Two generations of Holocene fans were mapped by Mc-

Calpin (1989), an early-middle Holocene set (af1) and late Holocene set (af2). These fans have not been numerically dated, but preliminary evidence from the nearby Wasatch fault zone suggests that many early-middle Holocene fans were deposited between about 4 thousand and 7 thousand years ago (Machette and others, 1987, 1992; Nelson, 1988; Personius, 1988, 1990). If the older ECFZ fans are of similar age, then the later faulting event should be older than about 4 thousand years. Such a minimum age is consistent with the degree of soil development on post-faulting colluvium (unit 45) and with the minimum TL age estimate of 2.5 ± 0.5 ka (3218).

Another method of estimating the age of the second faulting event is a quantitative analysis of soil properties. The loess-rich colluvial wedge from the earlier event (unit 44) has a well-developed buried soil consisting of B1k, B2k, and Ck horizons. The time represented by soil formation, plus the time required to deposit the colluvium, together should equal the total time elapsed between the first and second faulting events. If soil formation kept pace with loess deposition, then the time for cumulated soil formation alone should approximate the total time between fault events. To estimate the time represented by soil formation, total pedogenic clay and calcium carbonate in both soil profiles were measured (table 3). Estimating the percent clay and calcium carbonate present in the original parent material was difficult, because: (1) soil-forming processes had affected the entire deposit, due to cumulated profile development, and (2) it appeared that parent material was fining upward. A comparison of the estimated weight of pedogenic clay in the soil (table 3) with clay accumulation rates from other localities (Shroba, 1987) indicates that roughly 50 thousand years would be needed to form this soil. This age is directly contradicted by stratigraphic evidence, and radiocarbon and TL age estimates.

However, comparing the amount of clay in these two soils, which occupy a foot slope position, to soils on stable geomorphic surfaces (such as Shroba's) does not appear to be a valid comparison. Birkeland and others (1991) observed that foot slope soils are better developed than stable summit soils on landforms of a single age. An attempt was made to correct for "excess" eolian clay influx by subtracting that portion of clay which might have been added by eolian and slope wash processes. This procedure is experimental, and has not been previously described in the literature.

Elsewhere in the Bonneville basin, Pleistocene loess averages about 20 percent clay by weight (Ralph Shroba, personal communication). The increase in silt with decreasing depth in the colluvium is probably due to an increasing percentage of silty loess. The amount of excess silt (silt in the basal colluvium subtracted from silt in a given higher horizon), if of eolian origin, should have been accompanied by 20 percent as much clay. For example, in the B1k horizon there is an increase of 7 percent in the silt fraction and 6 percent in the clay fraction over the basal colluvium. If the 7 percent difference in silt all represents eolian input, then an increase of clay of 20 percent of that 7 percent (1.4 percent) may have occurred in the clay fraction. Thus, of the 6 percent of "excess" clay in the B2k, 1.4 percent may be attributable to eolian input with no contribution from weathering.

Using this methodology to correct for eolian-derived clay, pedogenic clay can be recalculated (table 3, last column). Com-

Table 3. Quantitative soil data, Bonneville trench.

UPPER SOIL HORIZONS	<2mm fraction			>2mm fraction(%)	primary ¹ silt(%)	eolian ² secondary silt(%)	estimated ³ eolian secondary clay(%)	primary+ ⁴ eolian secondary clay(%)	pedogenic ⁵ weathering clay(%)	bulk ⁶ density (g.cm ³)	horizon thickness (cm)	weight of ⁷ pedogenic weathering clay(g/cm ²)
	%sand	%silt	%clay									
A	31	42	12	15	16	26	5.2	13.2	-1.2	1.46	13	-0.23
Bw	39	29	14	18	16	13	2.6	10.6	+3.4	1.72	12	+0.70
B/C	39	26	13	22	16	10	2.0	10.0	+3.0	1.59	19	+0.91
Cox	37	17	7	37	16	1	0.2	8.2	-1.2	1.63	18	-0.35
C	40	14	8	38	16	-2	-0.4	7.6	+0.4	1.68	14	+0.09
												TOTAL = 1.12 g/cm ²
												CLAY ACCUMULATION RATE = 0.27 g/cm ² /ka ⁸
												AGE = 4.15 ka
LOWER SOIL HORIZONS												
B1k	41	32	18	10	25	7	1.4	13.4	+4.6	1.46	31	+2.08
B2k	49	29	13	9	25	4	0.8	12.8	+0.2	1.57	18	+0.06
Ck (upper)	55	24	13	9	25	-1	-0.2	11.8	+1.2	1.38	36	+0.60
Ck (lower)	63	26	11	0	25	1	0.2	12.2	-1.2	1.45	36	-0.63
												TOTAL = 2.11 g/cm ²
												CLAY ACCUMULATION RATE = 0.27 g/cm ² /ka
												AGE = 7.81 ka
												TOTAL OF BOTH SOILS = 3.23 g/cm ²
												TOTAL AGE OF BOTH SOILS = 11.96 ka

¹ calculated as the average silt content of the two lowest horizons.

² total silt minus primary silt.

³ assumed to be 20 percent of secondary silt (Shroba, 1987).

⁴ primary clay is the average clay content of the two lowest horizons.

⁵ total clay minus primary and eolian clay.

⁶ measured by paraffin coating and immersion.

⁷ percent pedogenic weathering clay multiplied by bulk density multiplied by horizon thickness.

⁸ from Shroba (personal communication, 1987).

paring the "corrected" total weight of pedogenic clay to Wasatch Front clay accumulation rates (Shroba, 1987) results in 12 thousand years of soil formation for the two superposed soils, when the actual time must be somewhat less than 15.5 thousand years. Using these same clay accumulation rates, the upper soil represents about 4 thousand years of soil formation, which is reasonably consistent with the TL age estimate of 2.5 ± 0.5 ka from the center of that soil.

The Provo Trench

Because the age of the later event at the Bonneville trench was poorly constrained, we excavated a second trench across a 1.2-meter-high (3.9 ft) scarp on the Logan Country Club golf course (figure 10). This trench, informally named the "Provo trench," was 12 meters (39 ft) long, 1.7 meters (5.6 ft) deep, and directly overlay the projection of the fault exposed in the 1930s road cut of U.S. Highway 89. The trenched fault scarp traverses an alluvial strath terrace 12 meters (39 ft) below the level of the Provo delta of the Logan River. Based on evidence from the Bonneville trench, this 1.2-meter-high (3.9 ft) scarp should represent only the latest faulting event; Swan and others (1983) also interpreted this scarp as a single-event feature.

The trench exposed the uppermost strath terrace gravels, which were divisible into three alluvial units (1a, 1b, and 1c in figure 11, and appendix B). Pedogenic carbonate coatings (Stage I-II of Gile and others, 1966) were found on the bottom and sides of clasts in the upper 50 to 60 centimeters (1.6-2.0 ft) of unit 1b, on both the upthrown and downthrown blocks. The three gravel units and calcareous soil are vertically displaced 1.15 meters (3.8 ft) down-to-the-west, compared to the vertical surface offset across the scarp of 1.2 meters (3.9 ft). A large crack-fill unit, mapped adjacent to the fault plane, is composed of carbonate-coated gravel similar to that of unit 1b, engulfed in a weakly organic sandy matrix. Abundant rootlets occur in the crack fill, following open void spaces. The steep orientation of the clasts in the crack fill, together with the carbonate rinds on the eastern side of stones, indicate that a block of gravel fell forward from the fault scarp free face soon after faulting, and lodged in the basal tension crack.

Overlying the crack fill is a thin deposit of gravelly, debris-facies colluvium (nomenclature of Nelson, 1987, 1992) with clast long axes oriented 25 to 35 degrees west. Oriented clasts suggest this unit (2b on figure 11) accumulated by angle-of-repose, gravity-fall deposition at the base of the retreating scarp free face. Unit 2b appears to overlie a buried soil organic horizon (unit A1/2a) on the downthrown block, although this contact is



Figure 10. Photograph of the fault scarp 1.2 meters (3.9 ft) high (center, between arrows) traversing the post-Provo strath terrace on the north side of Logan Canyon; view is to the east. The Provo trench was excavated at the location of the right pair of arrows.

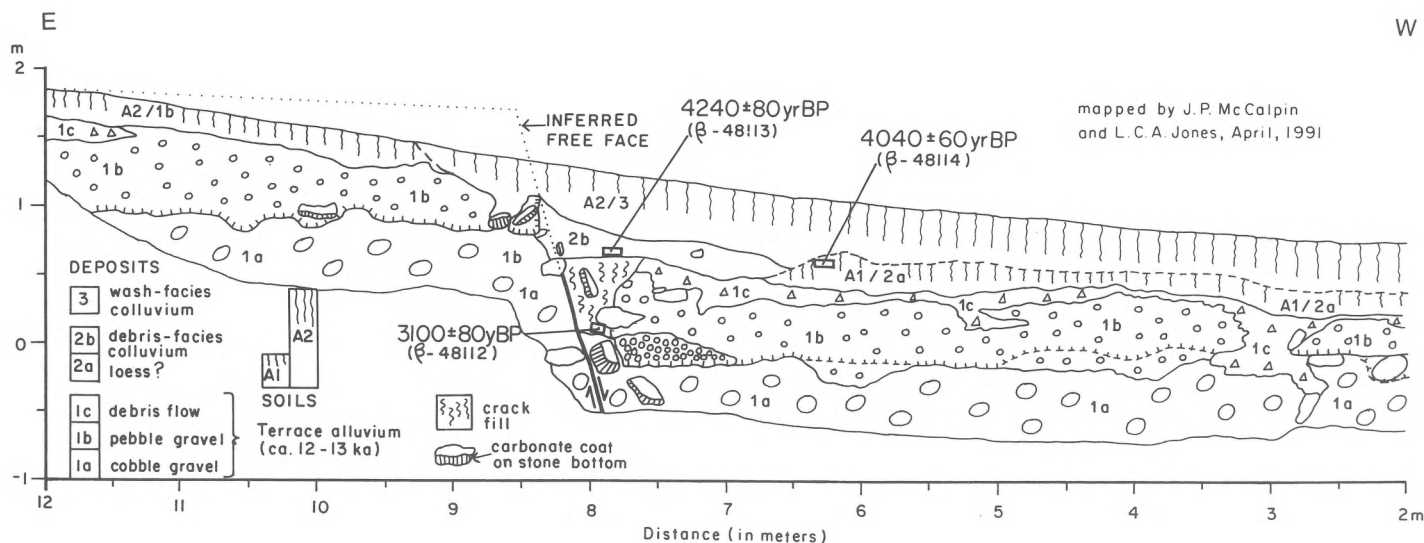


Figure 11. Log of the Provo trench across the central section of the ECFZ. Shaded area reflects organic soil horizons. Solid and dashed lines with hachures near the base of unit 1b mark the bottom of CaCO₃ deposition on clast bottoms. The nature of the contact between units 2b and A1/2a is obscure; it may be a facies contact between units of equivalent age. See appendix 2 for descriptions of units.

obscure in the trench. Overlying the debris-facies colluvium on the downthrown block is a sandy, clast-poor slopewash colluvium (wash facies) with a high organic content. This colluvium (unit A2/3) is a cumelic soil A horizon that is in depositional contact with gravels and soil (unit A2/1b) in the upthrown block.

Radiocarbon ages from three locations constrain the time of faulting. Organic matrix from the basal crack fill yielded an uncorrected ¹⁴C age of 3100 ± 80 yr B.P. (Beta-48112), whereas similar materials from the basal debris-facies colluvium and buried soil yielded ages of 4240 ± 80 yr B.P. (Beta-48113) and 4040 ± 60 yr B.P. (Beta-48114), respectively. These ages are

interpreted as follows. The crack fill age is 1,100 years younger than that of the overlying debris-facies colluvium. This stratigraphic reversal may be attributed to contamination of the crack fill with small modern rootlets, as previously described. The small age difference between the earliest debris-facies colluvium (4240 ± 80 yr B.P.) and the top of soil A1/2a (4040 ± 60 yr B.P.) may indicate that: (1) the basal debris contained A horizon material derived from the upthrown block that had a mean residence age of about 200 years at the time of faulting (see Machette and others, 1992, appendix), and/or (2) soil A1/2a continued to develop for about 200 years after faulting until finally buried by wash-facies colluvium. This age estimate of

4.0 to 4.2 thousand years for faulting is very similar to that predicted at the Bonneville trench (about 4 thousand years), based on the experimental quantitative analysis of the post-faulting soil.

Hidden Fault Traces

A fortuitous exposure near the center of the Provo delta of the Logan River, about 2 kilometers (1.2 mi) west of the range front, shows that faults may exist at a considerable distance valleyward from the main trace. A landslide occurred in 1984 on the south-facing slope cut by the Logan River through the Provo delta, roughly 200 meters (656 ft) southeast of the Ray B. West Building on the Utah State University campus (NW $\frac{1}{4}$, section 33, T. 12 N., R. 1 E.). The landslide head scarp cuts roughly halfway up this very steep hillslope and exposes deltaic gravels, sands, and silts offset 3.5 meters (11.5 ft) by a normal fault striking N55°-70°W, and dipping 55°-60°S (figure 12). The anomalous location of this fault, 2 kilometers (1.2 mi) west of the range front and in an area of historic landsliding, suggested it was possibly an old landslide shear. However, evidence supporting a tectonic versus a landslide origin is: (1) landslide head scarps should parallel the valley wall (strike N 70°E), yet the

fault strikes at a 50 degree angle to that trend, (2) the fault occurs on a ridge of deltaic material flanked by steep hollows to east and west; airphotos show no indication of Holocene landsliding on that ridge, and (3) the fault plane is a single sharp break with no tensional opening and no infilled debris in cracks, an unlikely situation if the feature were a landslide head scarp. Due to the limited exposure of this structure, it cannot be determined if it is a: (1) growth fault, (2) head scarp of an old lateral spread, such as at High Creek, or (3) a primary tectonic fault. Unfortunately, this exposure is the only one between mid-delta and the range front; many more such structures may exist in the deltaic pile.

No numerical ages constrain the ages of offset deposits, but correlation with Lake Bonneville deposits elsewhere suggests that the lower deltaic gravels represent the early stages of Provo delta deposition (13-14 thousand years?). No colluvial wedge is present near the surface, and the fault trace can be traced upward to within about 0.5 meters (1.6 ft) of the present ground surface, where active slope deposits begin. This geometry suggests that the displacement predates the formation of this steep hillside, which places it after 13-14 thousand years ago but before the stabilization of the present Logan River floodplain (early- to mid-Holocene?).

Summary Of Paleoseismology Of The Central Section

Geomorphic and trench evidence suggest that two surface-faulting events have occurred in the northern half of the central segment since the occupation of the Bonneville highstand shoreline. The earlier event resulted in about 1.8 meters (5.9 ft) of net displacement at the Bonneville trench site, but elsewhere displacement may have been larger (for example, where two-event scarp heights increase to 4.2 meters [13.8 ft], 0.5 kilometers (0.3 mi) south of the Bonneville trench; figure 5). The second event may have only caused 0.5 meters (1.6 ft) of displacement at the Bonneville trench site, but caused 1.2 meters (3.9 ft) of net displacement at the Logan Country Club golf course 1.2 kilometers (0.7 mi) to the north. The first event probably occurred between 13 thousand and 15.5 thousand years ago. The second event occurred about 4 thousand years ago. Maximum and minimum recurrence intervals based on numerical ages and soils are therefore 9 thousand and 11.5 thousand years, respectively, for the two events, with an average of 10.3 thousand years. The average recurrence time (10.3 thousand years) compared to the elapsed time since the latest event (4 thousand years) suggests that less than half of a "seismic cycle" has elapsed since the latest event, although only one recurrence interval is defined by this study. More detailed studies on the Wasatch fault zone (Machette and others, 1991, 1992) show wide variability in recurrence intervals on individual fault segments. Figure 13 summarizes the numerical age control on late Quaternary faulting events.

The 1930s road cut exposure (figure 6) showed that Bonneville prodelta sands near the bottom of the deltaic pile had been faulted 6.4 to 6.8 meters (21.0-22.3 ft), while Provo and post-Provo deposits were offset only about 1.1 meters (3.6 ft). Thus, the stratigraphic displacement on this fault plane that existed prior to the latest event was 5.2 to 5.6 meters (17.0-18.4 ft). This displacement may have arisen in two ways. First, it all may have

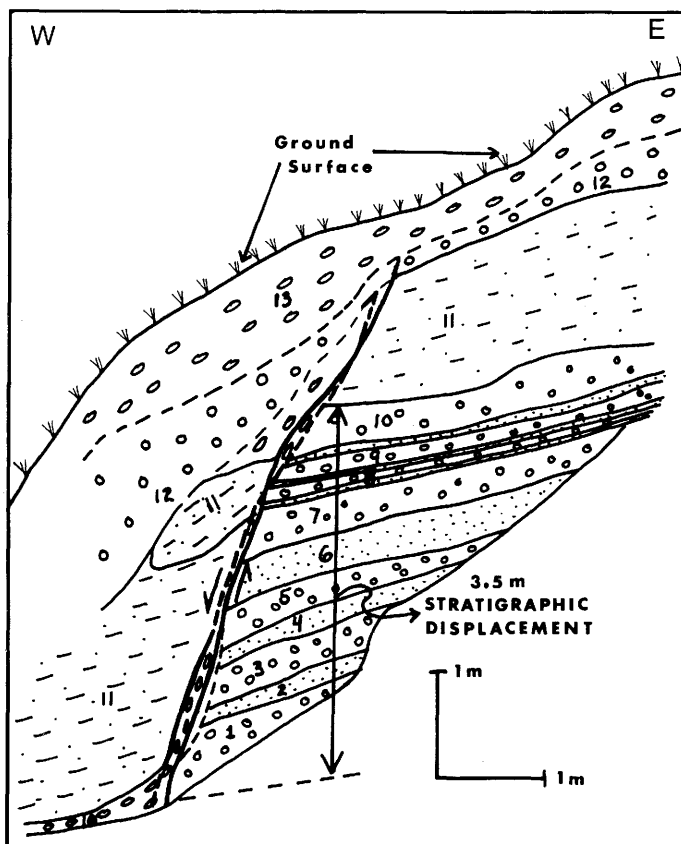


Figure 12. Sketch of "hidden" fault exposed in a landslide head-scarp near the Utah State University campus. Lithologic symbols: circles, gravel; dots, sand; dashes and dots, silt; elongated pebbles show clast fabric. Unit numbers are for correlation purposes; no detailed unit descriptions were made.

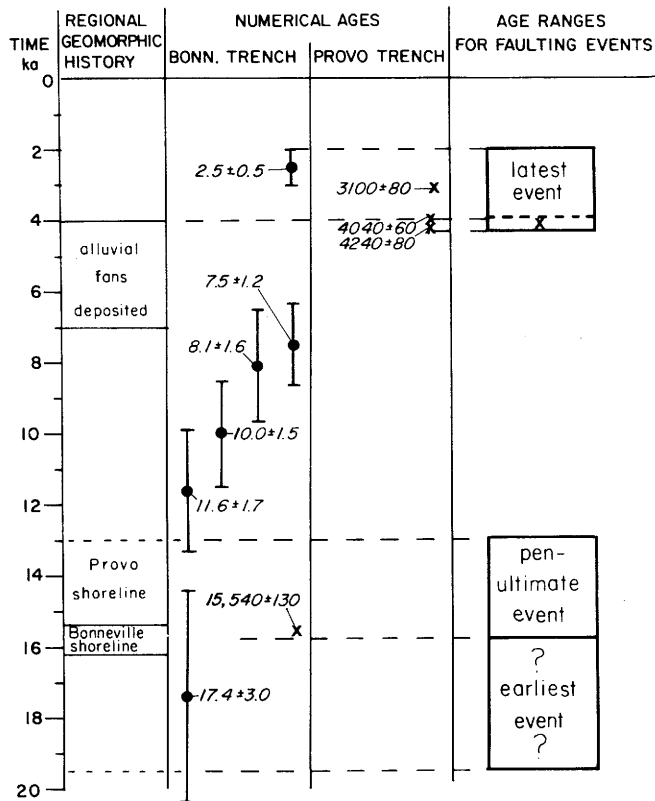


Figure 13. Diagram of inferred timing of faulting events on the central section of the ECFZ, as determined by regional geomorphic history, trenching, and numerical dating. Time is in radiocarbon and/or TL years, not corrected to calendar years. Heavy outlined boxes in the right column show inferred age ranges for faulting. The "X" in the box for the latest event indicates the preferred age estimate for this event.

occurred in the 13 to 15.5 thousand-year-old event recognized at the Bonneville trench. However, because stratigraphic displacement at the Bonneville trench during that event was only 3.1 meters (10.2 ft) (table 3), we would have to postulate that displacement in that single event increased from 3.1 meters (10.2 ft) to 5.2 to 5.6 meters (17.0-18.4 ft) in only 0.9 kilometers (0.5 mi) along strike. Admittedly, along-strike slip variations of this magnitude have been observed during historic normal fault surface ruptures (Wheeler, 1989, p.435). A second explanation is that the 5.2 to 5.6 meters (17.0-18.4 ft) stratigraphic displacement is the result of both the 13 to 15.5 thousand year event and an earlier event not observed at the Bonneville trench. This earlier event would have to predate the formation of the Bonneville highstand geomorphic surface. If we assume that displacement at the road cut was equal to that at the Bonneville trench during the 13 to 15.5 thousand year event, then as much as 2.1 to 2.5 meters (6.9-8.2 ft) of the displacement at the road cut could be attributed to this earliest inferred faulting event. I cannot distinguish between these hypotheses at present, but single-event displacements of 2 to 3 meters (6.6-9.8 ft) have commonly been inferred for the Wasatch fault zone (Machette and others, 1992), so a single pre-Bonneville-highstand event is likely.

This inferred earliest event must have occurred after deposition of prodelta sands at roughly 1,451 meters (4,759 ft) elevation, but before occupation of the Bonneville highstand shoreline. According to Currey and Oviatt (1985, figure 2), the Bonneville transgression reached 1,451 meters (4,759 ft) (elevation of the base of the road cut) by about 19.4 thousand years. However, because the area near the Bonneville shoreline at Logan Canyon has rebounded 14 meters (46 ft), (see section on Deformation of the Bonneville shoreline), the water actually reached the mouth of Logan Canyon at a pre-rebound elevation 1,437 meters (4,713 ft) about 19.5 thousand years ago. Thus, this earlier event suggested by net offset in the road cut may have occurred between 15.5 thousand and 19.5 thousand years ago. The recurrence time between this inferred event and the 13 to 15.5 thousand year event is less than 4 thousand years, which is considerably shorter than the 9 thousand to 11.5 thousand years between the latest two events. The shorter recurrence time during the filling of Lake Bonneville may reflect the response of the ECFZ to crustal loading and increased stresses and pore pressures, or may simply reflect irregular recurrence of faulting events.

Southern Section

The southern section of the ECFZ stretches from Blacksmith Fork Canyon to beyond the southern limits of this study (south of Avon, Utah). The fault is characterized by three parallel fault traces which bound a block of Tertiary Salt Lake Formation, similar to the northern section (figure 3). However, unlike the northern section, the more active trace south of Blacksmith Fork is the eastern trace at the base of a range front developed on Paleozoic rocks that is significantly steeper than along the northern section. The western traces, in contrast, are defined by an alignment of low saddles and stream channels cut into relatively soft Tertiary conglomerates and sandstones (McCalpin, 1989).

The eastern fault trace in the southern section is marked by an alignment of drainage segments and low saddles across the heads of pre-Bonneville pediments (Mullens and Izett, 1964; McCalpin, 1989). These pediments, termed the McKenzie Flat surface by Williams (1948), are assigned an early to mid-Pleistocene age because they: (1) overlie the Miocene-Pliocene Salt Lake Formation, but (2) are cut by the Bonneville highstand shoreline. At two locations between Hyrum Canyon and Paradise Dry Canyon, scarp profiles were measured across the fault trace (table 1). Pediment gravels are present on the downthrown block (maximum exposed thickness 9.5 m; 31 ft), but are very sparse on the narrow, eroded ridges of the upthrown block. Their scarcity implies that the upthrown surface has been eroded below its original position, which makes measured scarp heights minimum values for net vertical tectonic displacement. At each profile a zone up to 100 meters (328 ft) wide on the downthrown block has been back-rotated from the ambient pediment slope of 12 degrees to as low as 5 degrees. As a result, despite scarp heights of 20 to 30 meters (66-98 ft), the net surface offset from graphical projection is only 1.2 to 5.5 meters (3.9-18.0 ft).

Somewhat better expression of faulting is found along a short fault scarp to the south of the pediment saddles just described. Pre-Bonneville alluvium is offset by a well-preserved scarp just north of Paradise Dry Canyon (NE¼ section 1, T. 9 N., R. 2 E.). Scarp height is 15.8 meters (51.8 ft) and surface offset is 10.0 meters (32.8 ft). The 10 meter (32.8 ft) surface offset is considerably greater than the 1.2 to 5.5 meter (3.9-18.0 ft) offsets measured on the eroded pediments surfaces, but is less than their scarp heights of 20 to 30 meters (66-98 ft).

Although no fault scarps offset Bonneville-age and younger deposits in this section, shallow cuts in three locations show faulting of unconsolidated deposits. The northern location is immediately south of Blacksmith Fork Canyon where 12- to 15-meter-high (40-50 ft) cuts into Bonneville nearshore sands and silts were made to accommodate water tanks (figure 3, location 3). Near the western edge of the cut, sand and silt beds are offset by multiple down-to-the-west faults that dip about 35 degrees west. Cumulative offset across these fractures is at least 1.4 meters (4.6 ft). The location of the inferred main fault trace is roughly 10 to 15 meters (33-50 ft) farther west of the edge of this cut (based on projection from a large escarpment to the south), so these faults may represent either: (1) subsidiary faulting on a steep slope above the main fault, or (2) landslide head scarps with questionable tectonic significance. The anomalously low dip seems to argue for the latter interpretation, as does the absence of any fault scarps in young deposits in this section.

The second faulting locality is the south wall of a recent gully approximately 300 meters (984 ft) south of the first locality (figure 3, location 4). Here a paleosol developed on pre-Bonneville alluvium is offset a minimum of 2 meters (6.6 ft) vertically by multiple fractures. The fault does not appear to offset an overlying well-sorted gravel inferred to be the Bonneville transgressive gravel, nor overlying (Holocene) slopewash deposits. Although relations in this partly covered exposure are obscure, they suggest pre-Bonneville, but not post-Bonneville, surface faulting.

The southernmost location at which faults are exposed is a south-facing series of canal bank cuts on the north side of the East Fork, where the eastern trace of the ECFZ crosses the canal (figure 3, location 5). At two different locations within a 30-meter-wide (98 ft) zone, fault traces offset colluvium and buried soils deposited on a steep slope just above the Bonneville highstand shoreline. At the western cut, vertical calcite-filled shears in the lower colluvium and in a buried Ck horizon are truncated by the overlying younger colluvium (figure 14a). Individual beds in the lower colluvium could not be correlated, so net displacement could not be measured. At the eastern cut, two colluvial units are offset by at least 1 meter (3.3 ft) down-to-the-east (figure 14b). More shears may exist in the gully between these two canal cuts. It is not known if either of these faults is the main trace of the ECFZ, or if the main trace is located in the gully between cuts. The age of the faulted and unfaulted colluvium at both cuts is difficult to ascertain. The Bonneville highstand shoreline is so indistinct here that it is unclear whether the colluviums are older than, contemporaneous with, or younger than the Bonneville shoreline. Two TL age estimates (figure 14a) suggest that the lower, faulted colluvium is pre-Bonneville in age (45.6 ± 7.0 ka; Alpha-3210), while the upper, un-

faulted colluvium is roughly contemporaneous with the Bonneville transgression (25.8 ± 7.6 ka; Alpha-3209).

This age of latest faulting is compatible with the lack of fault scarps across deposits of the Bonneville lake cycle (11 to 30 thousand years ago) on the southern section. The age range is also roughly compatible with the age of latest faulting on the James Peak fault, estimated by Nelson and Sullivan (1987, 1992) at between 30 thousand and 70 thousand years ago (but nearer the younger age). Despite the poor age control, it appears that neither of the two paleoseismic events identified on the central section (about 4 thousand and 13 to 15 thousand years ago) produced observable rupture on the southern section. It is possible that the latest rupture on the James Peak fault may have also ruptured the southern section of the ECFZ, suggesting a maximum total rupture length of about 34 kilometers (20 mi).

Slip Rates And Recurrence

Slip rates and recurrence values for the southern section are highly speculative, because the age of the faulted pediments is not precisely known, and back-tilting and erosion complicate displacement measurements. If 10 meters (33 ft) is an typical displacement for pre-Bonneville deposits, which may range in age from 150 thousand years (Oxygen Isotope Stage 6) to 1 million years (early Pleistocene), the resulting slip rates would range from about 0.010-0.067 mm/yr (0.0004-0.003 in/yr). These very low rates contrast with the central section slip rates of 0.28 mm/yr (0.01 in/yr) during post-Bonneville time and 0.02-0.13 mm/yr (0.0008-0.005 in/yr) in the time since pre-Bonneville fan deposition. Recurrence intervals for the southern section can only be crudely estimated; if single-event net displacements of 0.5 to 1.5 meters (1.6-4.9 ft) are typical (as on the central section), then 10 meters (33 ft) of surface offset represents 7-20 surface-rupturing events in the last 150 thousand to 1 million years. Minimum and maximum average recurrences thus calculated would range from 7,500 years to 143,000 years respectively. A preferred recurrence estimate, based on a subjective geomorphic comparison of this section with other normal faults in the Basin and Range Province, would be in the range 15,000-30,000 years (for example, 10 1-m (3.3 ft) displacements in 150-300 thousand years) for this eastern splay. Based on the poorer topographic expression of the western splay, its recurrence interval may be even longer, or it may no longer be an active fault trace.

Paleoearthquake Magnitudes

Paleoearthquake magnitude on the ECFZ can be inferred from estimates of the maximum displacement per event and/or the length of surface rupture (Slemmons, 1982; Bonilla and others, 1984, worldwide data set; Khromovskikh, 1989). The earlier paleoearthquake on the central section, based on a minimum of 1.8 meters (5.9 ft) displacement at the Logan trench and a rupture length at least 8 kilometers (4.8 mi), or 16 kilometers (9.6 mi) if entire section ruptured, yields estimated paleomagnitudes of M_s 6.9 to 7.0 and M_s 6.0 to 7.1, based on the two

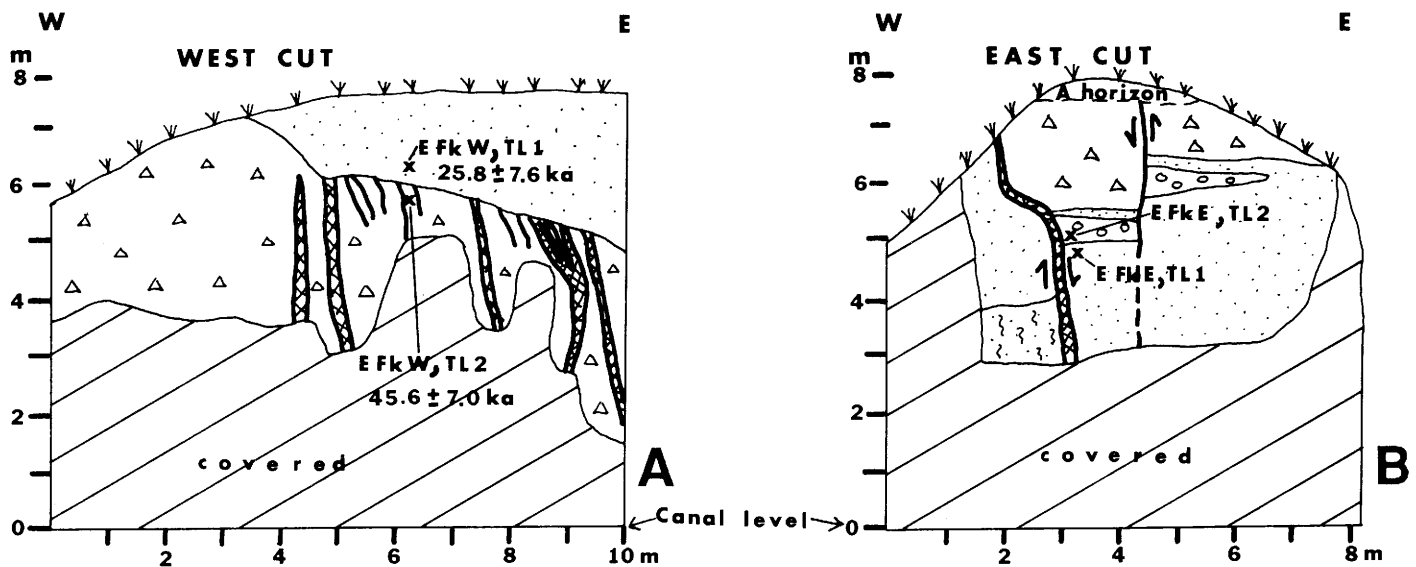


Figure 14. Sketches of fault traces on the southern section of the ECFZ, in canal cuts north of the East Fork (location 5 on figure 3). A) Triangles indicate faulted and sheared (cross-hatched zones) hillslope colluvium with abundant angular clasts and pedogenic CaCO_3 ; dots indicate finer sandy colluvium. TL age estimates bracket the latest faulting event in this cut between about 26 and 46 thousand years. B) All colluvial units in this exposure are faulted; two TL samples were collected (at labelled "x"s) but have not yet been dated. Triangles - stony colluvium; dots - fine sandy colluvium; open circles - gravelly channel deposit (small debris flow?); dots with vertical squiggles - sandy colluvium sheared and recemented with CaCO_3 . Because of the lack of surface expression of the ECFZ in this area, it is not clear whether any of these faults represent the main trace of the ECFZ.

rupture lengths cited above (table 4). The later event on the central section (maximum observed vertical displacement 1.4 meters (4.6 ft); unknown lateral extent) yields an estimated paleomagnitude of M_s 6.8 to 7.0 based on displacement. Field relations indicate that both of these ruptures did not extend beyond the 16-kilometer (9.6 mi) central section; this length of surface rupture corresponds to earthquakes of M_s 6.6 to 7.1 (table 4) and displacement of roughly 1.0 to 1.5 meters (3.3-4.9 ft) (Bonilla and others, 1984). Thus the displacements inferred for individual paleoseismic events on the central segment are compatible with segment length, and suggest events in the range of M_s 6.6 to 7.1.

The three-section subdivision of the ECFZ proposed in the Introduction is defined by changes in fault-zone complexity (change from a single trace to multiple traces) and by the absence of late Pleistocene fault scarps in the northern and southern sections. However, the structure of range-front faceted spurs is quite similar for the central and southern sections. Gravity data (Mabey, 1985) show that no subsurface gravity saddle exists between the central and southern sections, although on the Wasatch fault zone such saddles typically mark boundaries between seismogenic sections (Wheeler and Krystinik, 1988). These observations suggest that through much of late Cenozoic time the central and southern sections, which have a combined length of 44 kilometers (26 mi), and 51 kilometers (31 mi) if the James Peak fault is included, may have acted as a single seismogenic section. However, late Pleistocene fault scarps on the central section do *not* extend into the southern section. Rupture terminations indicate that in the last two ruptures the central section has acted as a seismogenic section, but over the entire Quaternary the central/southern section boundary may have been nonpersistent. In contrast, the boundary between the

central and northern sections is marked by a gravity saddle in Cache Valley (Mabey, 1985) and by a significant decrease in the complexity and number of range-front faceted spurs. This boundary may be a persistent segment boundary between the long central segment and the northern section composed of one or more seismogenic segments.

The hypothetical multi-segment ruptures, such as a 25 thousand to 45 thousand year event involving the James Peak fault and southern section of the ECFZ (length 34 km; 20 mi) or a combined central-southern section rupture (length 44 km; 26 mi) imply larger earthquakes. Nelson and Sullivan (1987, 1992) noted that the discrete displacements of 1.8 meters and 2.4 meters (5.9 ft and 7.9 ft) inferred on the James Peak fault were anomalously large for the 7 to 10 kilometer (4.2 to 6 mi) length of the fault, and hypothesized that such events also ruptured the southern section of the ECFZ. Displacements of 1.8 to 2.4 meters (5.9-7.9 ft) are associated with surface rupture lengths of 39 to 45 kilometers (23-27 mi) (Bonilla and others, 1984), lengths which are more similar to the combined James Peak fault-southern section length of 34 kilometers (20 mi) than to the individual lengths of either section (10 km and 24 km; 6 mi and 14 mi). These larger earthquake events (M_s 7.2) may have recurrence intervals of 50 thousand years or more (Nelson and Sullivan, 1992).

DEFORMATION OF THE BONNEVILLE HIGHSTAND SHORELINE

Past studies of the elevation of the Bonneville-highstand shoreline (Crittenden, 1963; Passey, 1984) have shown the usefulness of this once horizontal datum in deciphering regional-

Table 4. Inferred magnitudes of paleoearthquakes on the central section of the ECFZ.

	DISPLACEMENT PER EVENT		ESTIMATED SEISMIC MOMENT ¹	INFERRED MOMENT MAGNITUDE ²			
	Vertical (m)	Net Slip ⁴ (m)	Mo (dyne-cm)	Mw	M _s ³ from Bonilla et al, 1984	M _s ³ from Slemmons 1982	M _L from Khromovskikh 1989
Earlier Event at Trench	1.6	1.8	1.88x10 ²⁶	6.8	7.0 ⁵	6.9 ⁶	
Later Event at Trench	0.9	1.0	1.04x10 ²⁶	6.6	6.8 ⁵	6.7 ⁶	
Later Event on Provo delta	1.4	1.6	1.69x10 ²⁶	6.8	7.0 ⁵	6.8 ⁶	
Probable Maximum Paleoevent	2.1 ⁹	2.4	2.53x10 ²⁶	6.9	7.1 ⁵	6.9 ⁶	
	LENGTH OF RUPTURE (km)						
Minimum	8				6.7 ⁷	6.0 ⁸	6.6 ¹⁰
Probable	16				7.0 ⁷	6.6 ⁸	7.1 ¹⁰

FOOTNOTES

¹ Mo=MAD, assuming: $M=3 \times 10^{11}$ dyne/cm² (Arabas and others, 1979);

A=area of fault plane, assuming length of 20 km, depth of 15 km, dip of 60°; D=displacement (net slip)

² Mw=2/3 Mo -10.7 (Hanks and Kanamori, 1979)³ Inferred from regression of M_s on log of displacement from historic earthquakes⁴ Assuming 60° dip of causative fault at seismogenic depths⁵ Normal fault data only, ordinary least squares regression; M_s=6.71+0.741 log d(m)⁶ Normal fault data only; M_s=6.668+0.75 log d(m)⁷ Plate interior faults only, ordinary least squares regression; M_s+6.02+0.729 log L(km)⁸ Normal fault data only; M_s=0.809+1.341 log L(m)⁹ Probable maximum per-event displacement in late Quaternary time, estimated by partitioning the maximum observed vertical surface displacement (4.2 m) equally between two events.¹⁰ Faults of "ancient platforms rejuvenated in Cenozoic"; M_L=5.45+1.25 log L (km)

scale crustal rebound chronologies. However, the datum can also be used to detect relative motion of mountain blocks and valleys separated by Holocene normal faults (McCalpin and Garr, 1984; McCalpin and others, 1987, 1992). Because fault scarps were present on only a small fraction of the length of the ECFZ, an independent method of detecting Quaternary uplift was needed. Specifically, I wondered if the Bonneville highstand shoreline had the same elevation within each of the three fault sections as it roughly paralleled the ECFZ for 56 kilometers (34 mi). Abrupt changes in shoreline elevation across section boundaries would indicate that, even though scarps were not visible, differential movement of the mountain blocks had occurred.

The experimental design had several components. First, shoreline elevation was determined by surveying along the eastern side of Cache Valley. Second, shoreline elevations were plotted along strike. Finally, residual anomalies were compared to section boundaries in an attempt at correlation.

Methods

Surveying of the Bonneville shoreline was carried out by a three-man field crew over seven weeks during the summer of 1986. Two surveying methods were initially employed. In the first method, bench marks in the valley west of the shoreline were

occupied, then a traverse was performed with a Leitz TM-20H theodolite and RED-2 Electronic Distance Meter from bench mark to survey stations along the range front, and back to another bench mark in the valley. In the following discussion, surveyed elevations are quoted in feet first, because bench-mark elevations are defined in feet, and all field computations were performed in feet.

Survey station elevations were computed by trigonometric levelling, with closure errors distributed among stations based on the length of traverse legs connecting the stations. Survey stations along the range front were typically 0.5 to 1.5 kilometers (0.3-0.9 mi) apart. Survey stations were located on low-gradient shoreline platforms if possible; if not, then some nearby position was used. Vertical closure of such traverses was as low as 0.11 ft (0.03 m) over a horizontal distance of 45,800 feet (14 km), but averaged about 0.9 ft (0.3 m) for the eight survey station loops (table 5). Because such survey traverses along the range front were logistically difficult and time consuming, a second, faster method was tested.

In the second method, stations valleyward of the shoreline were surveyed using traverses between bench marks. Typically these stations (hubs) would be 0.5-1.0 kilometers (0.3-0.6 mi) west of the Bonneville-highstand shoreline, located near a road. From these hub stations, radial sights would be made on several shoreline positions. The elevation of the shoreline position would then be calculated trigonometrically, based on the vertical angle and slope distance from the hub survey station (below the shoreline) to the profile control point (on the shoreline). All radial sights were doubled by reversing the theodolite, and the two vertical-angle measurements were averaged.

The surveyed elevation was related to the shoreline elevation in the first method by measuring a topographic profile across the shoreline which included the survey station. This profile was measured by laying a 4.5-meter (14.8 ft) extendable fiberglass stadia rod on the ground and measuring local ground slope with

an Abney level, in a manner similar to fault scarp profiling (see Bucknam and Anderson, 1979). Field values for rod length and slope were plotted into shoreline profiles on a dot-matrix printer using the LOTUS spreadsheet package. One of the section junctions in the profile represented a surveyed control point. The control point might be below the shoreline platform, on it, or above it, depending on maximum visibility for sighting the next station on the traverse. In the second method (employing radial sights), a shoreline profile was also measured, one point on which was denoted as a profile control point. This profile control point was then sighted from the hub station and its elevation was calculated.

To test the accuracy of such long radial sights for determining profile control point elevation, both surveying methods were used on the same traverse (a 3 km [1.8 mi] stretch between Green Canyon and Logan Canyon). Eight profile control points were surveyed for vertical elevation by the two methods (table 6, profiles 1-8). The minimum and maximum discrepancy between profile control elevations of the two methods was +0.02 foot (0.006 m) and +1.60 feet (0.5 m) respectively, with an average of +0.76 foot (0.23 m). Radial sights typically yielded a control point elevation roughly 0.75 foot (0.23 ft) higher than the shoreline traverses. However, it was felt that the radial method was accurate enough for purposes of detecting tectonic warping, considering that: (1) the magnitude of suspected anomalies was thought to be in the 1.5 to 3 meter (4.9-9.8 ft) range, similar to heights of post-Bonneville fault scarps, and (2) the 0.76 foot (0.23 m) inaccuracy was smaller than uncertainties resulting from profile projection to determine paleo-water level (discussed in the next paragraph). Accordingly, most of the shoreline profile control points were surveyed by the radial method, except where it was easy to site a survey station on the shoreline itself.

The largest error in determining shoreline elevation came from relating the surveyed profile control point elevation to the

Table 5. Summary of control data for survey traverses of the Bonneville highstand shoreline.

Traverse ¹	Start ²	End ³	Horizontal Distance (ft)	Vertical Distance (ft)	Vertical Closure Error (ft)	Number of Stations
SR 1-7	Green Canyon	Crow BM "C"	44,735.27	3,241.10	+2.87	9
SR 8-17	Crow BM "C"	BM A338	66,655.11	3,008.32	-0.81	12
Hyrum area	BM "G", Black-smith Fork	BM "A"	11,890.10	359.94	+0.29	4
	BM "A"	BM "B"	15,354.63	690.41	+0.63	3
	Hy-5	Hy-7 (BM"D")	16,763.45	339.32	+1.10	3
	Hy-7	Hy-9 (BM"G")	9,726.57	532.91	-0.55	3
	Hy-9	BM 5073	12,684.94	388.19	-1.06	3
P	BM "G"	VABM	45,808.39	1,198.48	-0.12	11
		TOTALS	223,618.46 (42.4 mi)	9,758.67	TOTAL= 7.42 ft AVERAGE= 0.93 ft	48

¹ Traverse abbreviations depict the general area of the traverse; SR-Smithfield-Richmond, H-Hyrum, P-Paradise

² Bench marks are informally named, keyed to field survey maps in the author's possession.

³ Cumulative horizontal distance on the traverse.

⁴ Cumulative vertical distance changes on the traverse.

⁵ Computed closure error upon arrival at the end bench mark.

Table 6. Comparison of the closed traverse vs the radial sight method (all elevations in feet above sea level).

Profile Control	Shoreline Traverse Method ²	Radial ₃ Sight Method ³	Difference ⁴ (ft)
Pro-1	5126.85	5127.90	+1.05
2	5127.38	5127.94	+0.56
3	5126.10	5126.90	+0.80
4	5125.20	5126.80	+1.60
5	5125.95 ⁵	5125.88	-0.07
6	5117.85 ⁵	5118.82 ⁵	+0.97
7	5126.77	5126.79	+0.02
8	5126.93	5127.94	+1.01

AVERAGE= 0.76 ft absolute

¹ Pro. 1 is the northernmost point, Pro. 8 is the southernmost; actual locations are shown on field survey maps (1:24,000) in the author's possession.

² Elevations based on including the profile control point within a survey control traverse, as explained in the text.

³ Elevations based on making radial sights to the profile control point from a control station located 0.5-1.0 km away, as explained in the text.

⁴ The elevation from the radial sight method minus the elevation from the shoreline traverse method. On 6 of 8 points, the radial method gave a slightly higher elevation.

⁵ Anomalously low shoreline elevation by both methods; cause not determined, but possibly due to slumping.

actual elevation of the Lake Bonneville mean water surface occupied roughly 15,000 years ago. The relation of mean water level to shoreline geomorphic elements is not perfectly consistent, even on modern shorelines. Rose (1981) tabulated data relating mean sea level to elevation of the shoreline angle on various types of coasts, and concluded that for high-energy, swash-dominated shorelines, the shoreline angle approximated the mean water level. Most of the Bonneville shoreline on the eastern side of Cache Valley is erosional, and large gravels on shoreline platforms suggest a high-energy environment. Large-scale patterns of bars and spits around the valley also reveal strong southward longshore drift at the Bonneville shoreline, and much more erosion on west-facing than on east-facing shores. These two facts imply that prevailing winds in Bonneville time were from the northwest (as they are today), making the west-facing shorelines at the base of the Bear River Range subject to high-energy wave action. Thus, for erosional shorelines, it is presumed that the shoreline angle approximates the mean water level, ± 0.5 meters (1.6 ft) (Rose, 1981).

At several locations along the shoreline, spits and baymouth bars developed, which in turn cut down on wave energy impacting the range front, and led to poorly developed erosional shorelines. Twelve survey points were located on spit and bar crests (dashed line in figure 15), but these measurements are typically 3 meters (10 ft) higher than elevations from adjacent erosional shorelines. D.R.Currey (personal communication, 1986) has observed that Bonneville baymouth bar gravels seem to be piled up by storm wave action to an elevation higher than the mean water level. In contrast, the two survey points measured on spit crests (not shown on figure 15) were lower than adjacent erosional shorelines. This probably occurred because the spit crests sloped gently downhill away from their junction

with an erosional shoreline, and this slope was too gentle to be noticed in the field.

Assuming that the shoreline angle approximated the mean water level of Lake Bonneville, the next task was to find the shoreline angle. Previous studies of marine terraces (Bradley and Griggs, 1976) used geophysics to locate the bedrock shoreline platform and the shoreline angle under a cover of terrace deposits and colluvium. At many places in Cache Valley, bedrock protrudes through erosional shoreline platforms, so thick platform cover is generally not a problem. However, the original shoreline angle of all erosional shorelines is presently covered with a wedge of colluvium deposited in the last 15 thousand years. We use the method of McCalpin and others (1992), by projecting the angle of the wave-cut cliff (typically 35 to 40 degrees) downward under the colluvium, while projecting the angle of the shoreline platform (typically 3 to 8 degrees) up under the colluvium, to determine the intersection of those two planes. This procedure assumes that the wedge of colluvium can be approximated as having two planar contacts, and that it rests directly on the original shoreline angle. We have no direct evidence that this is true in Cache Valley. However, in Pocatello Valley (80 km or 50 mi to the northwest) McCalpin and others (1987, 1992) dug two backhoe trenches across Bonneville shorelines which had been covered by Holocene colluvium. In each case the top of the beach gravel lens exposed in the trench was less than one foot (0.3 m) lower than the projection of platform and cliff angles. Based on that evidence, we conclude that the estimated shoreline-angle elevation based on projection from shoreline profiles is within 1 foot (0.3 m) of the true shoreline angle. This true shoreline angle should be within 0.5 meters (1.6 ft) of the mean water level of Lake Bonneville.

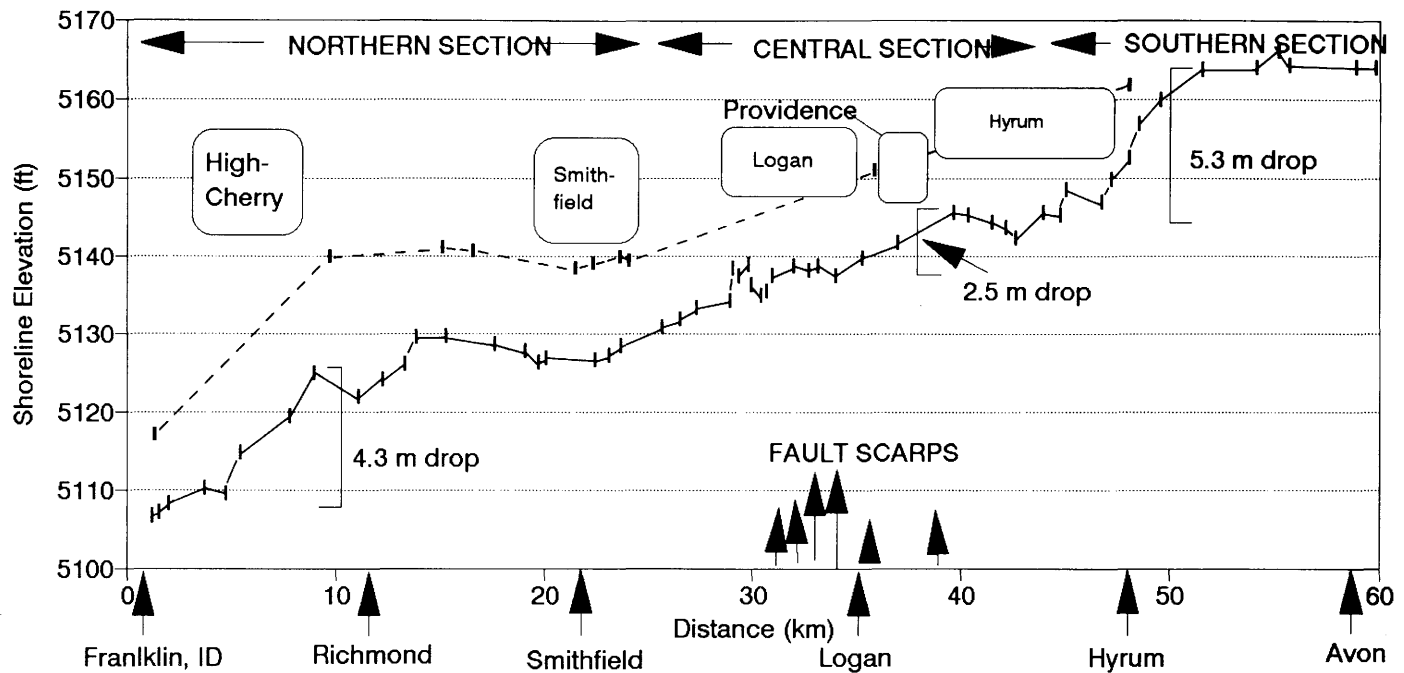


Figure 15. Longitudinal profile of the Bonneville highstand shoreline along the Bear River Range front, parallel to the ECFZ. Vertical bars represent estimated elevations of shoreline angles of erosional shorelines, projected under colluvial cover as described in the text; bar heights indicate measurement uncertainty. Dashed line indicates elevations of bar crests. The extent of post-Bonneville-highstand fault scarps is shown by arrows under "FAULT SCARPS"; arrow length depicts net vertical displacement to scale. Labelled boxes show areal extent of deltas deposited at the Provo level (see figure 1).

To total the uncertainties related to shoreline elevation, we must add the survey station closure error (± 0.9 ft; ± 0.27 m), to the radial sight error (within 0.76 ft, or ± 0.38 ft; ± 0.11 m), to the shoreline angle projection uncertainty (± 1.0 ft; ± 0.3 m), to the uncertain relation between the shoreline angle and mean water level (± 1.6 ft or ± 0.5 m). These errors, if they all sum, add to a combined uncertainty of 3.9 ft (1.2 m) possible for each surveyed shoreline elevation point. This finding was disturbing, because I anticipated looking for elevation anomalies of 1.5 to 3.0 meters (5-10 feet) due to tectonics, and the total uncertainty was near that range. Fortunately the major anomalies actually detected have amplitudes of 2.5 to 5.3 meters (8.2-17.4 feet), considerably greater than combined error.

Results

Longitudinal Profile

A total of 82 shoreline elevations were measured along the 56-kilometer (34 mi) distance from Avon, Utah northward to the Idaho state line. A longitudinal elevation profile (figure 15) shows a general decrease in shoreline elevation from 5,165 feet (1,575 m) at Avon, to 5,107 feet (1,557 m) at the Idaho-Utah border. This slope of 1.7 ft/mile (0.33 m/km) is less than the maximum slope due to isostatic rebound elsewhere in the Bon-

neville basin, because the traverse is not exactly at right angles to rebound contours (Crittenden, 1963). Notably, the 58 feet (18 m) of shoreline elevation drop along the traverse is not uniformly distributed along strike. Most of the drop occurs in three short reaches totalling less than 10 percent of traverse length. The southernmost drop (17.4 ft; 5.3 m) occurs in a 4-kilometer (2.4 mi) stretch south of the mouth of Blacksmith Fork. Immediately south of the Logan delta the shoreline drops 8.2 feet (2.5 m), while the northern drop (14.1 ft; 4.3 m) occurs in a 2.5-kilometer (1.5 mi) stretch north of Richmond. The remaining anomaly is a broad sag in shoreline elevations centered near Smithfield, where the shoreline tilts slightly southward instead of northward. All elevation data are from similar, high-energy erosional shorelines.

If shoreline anomalies were a result of differential tectonic movement across seismogenic segment boundaries, we might expect to find them: (1) across the mouth of Blacksmith Fork (central/southern segment boundary), and (2) across the mouth of Green Canyon (northern/central segment boundary). The center of the southern anomaly is well south of Blacksmith Fork, the Logan delta anomaly is in the center of the central segment, and the northern anomaly appears within the northern section. There is no observable shoreline deflection across either section boundary. In addition, shoreline drops are not abrupt (as might occur with tectonic decoupling of sections) but span a horizontal distance of 2.5 to 4 kilometers (1.5-2.4 mi), which suggests broad, monoclinical folding rather than abrupt offset on faults.

If shoreline anomalies were the result of direct surface faulting, they should coincide with the limits of post-Bonneville fault scarps, which are restricted to the center of the central section. As shown in figure 15, no shoreline deflections occur where post-shoreline faulting of up to 4.2 meters (13.8 ft) has been documented in the central section. Because all fault scarps occur downslope of the Bonneville-highstand shoreline, the shoreline is carved on the upthrown fault block in the central section. If the shoreline carved into the upthrown block in the central section had been uplifted by surface faulting, one might expect it to be higher (by the height of fault scarps) than unfaulted shorelines in the northern and southern sections. Figure 15 shows this is clearly not the case - the shoreline in the central section is actually slightly lower than it should be between Hyrum and Smithfield, and no shoreline deflection occurs where fault scarps terminate. Because up to 4.2 meters (13.8 ft) of post-Bonneville fault offset has occurred in the central segment, but shoreline elevation has not been affected, one may infer the absolute sense of movement in the segment during the latest two faulting events; the upthrown (mountain) block remained stationary, while the downthrown (valley) block slipped down. Such a geometry has been geodetically documented for the 1983 Borah Peak earthquake (upthrown block moved up 20 centimeters [0.6 ft], downthrown block moved down 1.2 meters [3.9 ft]; Stein and Barrientos, 1985) and has also been inferred from Bonneville shoreline surveying evidence in Pocatello Valley, Idaho (McCalpin and others, 1992). However, if shoreline anomalies are not related to faulting, an alternative cause must be sought.

Large Bonneville and Provo delta complexes occur near each of the shoreline elevation anomalies (figures 1 and 15). This coincidence suggests that depositional loading may be responsible for the shoreline deflections. Along the range front, the largest depositional piles which were rapidly loaded onto the floor of Lake Bonneville are (in order of decreasing area): (1) at Hyrum (combined Little Bear River - Blacksmith Fork delta, area 20.9 km²; 8.2 mi²), (2) Logan (Logan River delta, area 7.1 km²; 2.8 mi²), (3) Smithfield (Summit Creek delta, area 5.7 km²; 2.2 mi²), (4) north of Richmond (Cherry Creek - High Creek deltas, area 4.1 km²; 1.6 mi²), and (5) Providence (Spring Creek delta, area 3.7 km²; 1.4 mi²). Well logs from the Logan delta (Shannon and Wilson and Akbabian Associates, 1980) indicate that the deltaic piles are roughly 100 meters (328 ft) thick, and are composed of gravel overlying deeper water sand and silts.

The volume of each delta was calculated by multiplying its area times an assumed 100-meter (328 ft) thickness. Specific gravities from the Logan delta well, based on measured dry densities, were used to convert volumes into total weights for a typical 2-kilometer-radius (1.2 mi), 100-meter-thick (328 ft) delta. The resulting data (table 7) were input into a model of an elastic beam overlying a ductile half-space subjected to a point load equal to delta weight. The local crustal model used to represent the beam was derived from Smith and Bruhn (1984), who propose a rigid 10-kilometer-thick (6 mi) crust (the beam) characterized by abundant earthquakes, overlying a more ductile crust (the half-space). Depending on the Young's modulus and Poisson's ratio assigned to the beam, the model predicted deflections from loading of 1 to 7 meters (3.3 ft to 23 ft) (table 7). This

range is within the amplitude range of observed shoreline deflections. However, the radius of such loading deflections is roughly 30 to 70 kilometers (18-42 mi), which is much greater than the full width of shoreline elevation anomalies. The two large anomalies seem to match best with the model of thinnest, most yielding and weakest crust.

Transverse Profile

Elevations of the Bonneville highstand shoreline were also determined roughly perpendicular to the strike of the ECFZ by surveying a traverse 3.5 kilometers (2.1 mi) up the East Fork east of Avon (figure 3). At the Bonneville highstand, lake water extended up the East Fork as an estuary as far east as the eastern splay of the ECFZ. Shorelines become progressively more subdued upstream, probably because wave energy decreased upvalley in the estuary. It was hoped that the shoreline could be traced across the eastern splay to look for evidence of abrupt offset; unfortunately, no shorelines east of the fault were well expressed enough to survey. However, eight shoreline elevations between Avon and the eastern splay were measured and are plotted on figure 16. Between the main Bonneville shoreline at Avon and 1.5 kilometers (0.9 mi) upstream, the shoreline apparently loses about 4.6 meters (15 ft) in elevation. The two easternmost profiles (29 and 30 in figure 16) were surveyed on poorly preserved, small embankments that could be either shoreline platforms or alluvial terraces, thus the shoreline correlation is queried to them on figure 16. Shoreline point 30, on the upthrown side of the fault, is 2.1 meters (6.9 ft) higher than shoreline point 29, about 200 meters (656 ft) to the west on the downthrown block. However, other adjacent shoreline elevations in this estuary (for example, 22 and 31, 27 and 26, 24 and 28, figure 16) vary by at least this amount, so the anomaly cannot be definitely attributed to tectonic uplift on the ECFZ. More troublesome, however, is the downward trend of the shoreline as it is traced upstream (southeast) toward the ECFZ. Regional isostatic rebound contours are roughly parallel to this traverse so the anomaly cannot be attributed to regional causes. The meager deltaic deposition in the estuary should have, if anything, produced a depositional surface which had a gentle downstream gradient, not an upstream gradient as observed.

The trend shown in figure 16 appears similar to geodetic profiles of downthrown block deformation following the 1959 Hebgen Lake earthquake (Myers and Hamilton, 1964). Keaton (1987) analyzed models for regional-scale tilting of downthrown normal fault surfaces in M 7 events. The profile in figure 16 is similar to the shape and amplitude of both observed and modeled deformation after historic events. However, this interpretation raises another problem. Evidence presented previously indicated that Bonneville deposits on the southern section were not displaced (except at one ambiguous location). Tectonic tilting of the shoreline towards the fault, however, certainly requires post-Bonneville faulting. Due to the poor preservation of shorelines and lack of fault exposures in the East Fork, it is doubtful that this dilemma can be resolved. Certainly no Holocene surface-faulting events have occurred on the southern section, as indicated by unfaulted Holocene alluvium in drainages, so the only possible post-Bonneville rupture would be a near correlative to the 13 to 15 thousand year event dated

Table 7. Input data for rheologic modeling of Bonneville highstand shoreline deformation.

Model Run ¹	Thickness (km) ²	Beam Input Parameters			Output Parameters		
		Young's Modulus ³	Poisson's Ratio ⁴	Deltaic Mass ⁵ (10 ¹² kg)	Beam Subsidence ⁶ (m)	Radius of Subsidence ⁷ (km)	
1	7	1 x 10 ¹¹	0.25	1.37	1.94	60	
2	10	1 x 10 ¹¹	0.25	1.37	1.49	100	
3	15	1 x 10 ¹¹	0.25	1.37	1.09	135	
4	7	1 x 10 ¹¹	0.25	2.75	3.88	70	
5	10	1 x 10 ¹¹	0.25	2.75	2.90	100	
6	15	1 x 10 ¹¹	0.25	2.75	2.19	130	
7	7	1 x 10 ¹⁰	0.1	1.37	3.50 ⁸	35 ⁸	
8	10	1 x 10 ¹⁰	0.1	1.37	2.68	50	
9	15	1 x 10 ¹⁰	0.1	1.37	1.98	70	
10	7	1 x 10 ¹⁰	0.1	2.75	7.05 ⁸	40 ⁸	
11	10	1 x 10 ¹⁰	0.1	2.75	5.39	50	
12	15	1 x 10 ¹⁰	0.1	2.75	3.97	70	

¹ All models are based on the equation for beam deflection under a point load cited by Hetenyi (1946). The substrate under the beam is assumed to be a ductile substance of density 3.0 g/cm³.

² Beam thickness estimates follow estimates of the thickness of the brittle (seismogenic) part of the crust by Smith and Bruhn (1984).

³ Young's Modulus of the beam (= the brittle crust) is assumed from typical values for upper crustal rocks (Johnson, 1970).

⁴ Poisson's Ratio of the beam (= the brittle crust) is assumed from typical values for upper crustal rocks (Johnson, 1970).

⁵ Deltaic masses reflect two sizes. The larger size (a cylinder with radius 2 km, thickness = 100 m, volume = 1.25 km³), that approximates the larger Hyrum and Logan deltas, and a smaller size with 50 percent as much volume, to account for the smaller deltas and uncertainties in thickness values. Assumed bulk density of deltaic material is 2.2 g/cm³. Estimated volumes and weights for deltas are 2.1 km³ and 4.6 x 10¹² kg for the Hyrum delta, 0.7 km³ and 1.5 x 10¹² kg for the Logan delta, and 0.4 km³ and 0.9 x 10¹² kg for the High Creek/Cherry Creek delta.

⁶ Maximum vertical subsidence of the beam underneath the center of the applied point load.

⁷ Horizontal distance from the center of subsidence to its lateral limits.

⁸ Output values that most closely match the observed vertical subsidence and radius of subsidence result from a thin (7 km) brittle crust composed of weak, yielding rocks. This conclusion follows that of Smith and Bruhn (1984), that the brittle crust in the eastern Basin and Range is thinner and more ductile than average.

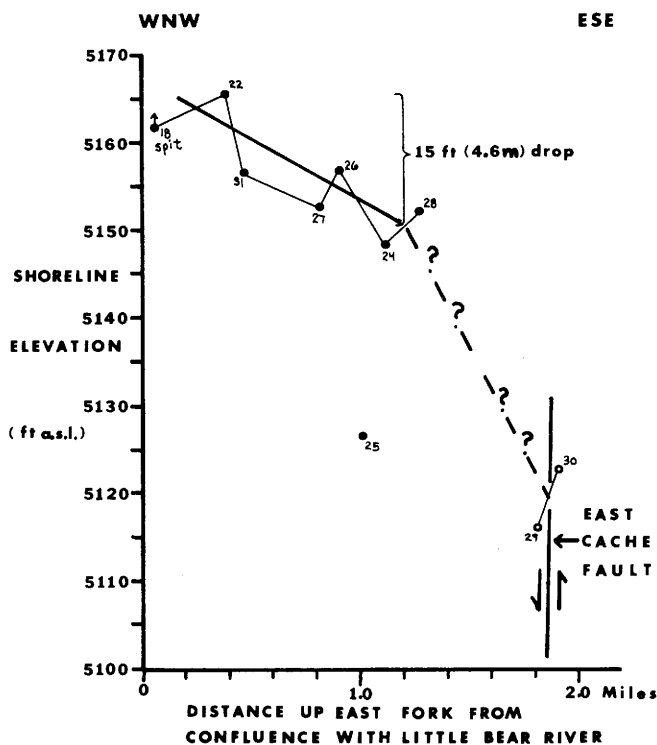


Figure 16. Transverse profile of the elevations of the highstand shoreline of the Bonneville lake cycle, perpendicular to the southern section of the ECFZ at East Fork. Survey point 25 may have been affected by slumping. Survey points 29 and 30 are on small terrace remnants that may postdate the Bonneville highstand, so correlation with other survey points is queried. The overall trend of survey points on the unambiguous Bonneville shoreline (points 18-31) is a 4.6 meter (15 ft) drop to the east, or upstream in the East Fork valley.

on the central segment. This dilemma might be solved by detailed trenching studies on the southern section that were beyond the scope of this investigation.

TECTONIC GEOMORPHOLOGY OF THE BEAR RIVER RANGE FRONT

The tectonic geomorphology of the Bear River Range front above the ECFZ was studied for evidence of tectonic trends that predate the late Quaternary. Direct evidence for fault history in pre-Bonneville time is scarce because the fault trace is mainly covered by Bonneville lacustrine deposits. With relatively weak evidence for fault segmentation from fault scarps and shoreline surveying, it was hoped that more convincing long-term evidence for segmentation would be seen in the structure of range-front facets and drainage-basin morphology.

Overall Physiography

The Bear River Range front is remarkably linear at a small scale (80 km; 48 mi distance), but exhibits topographic divisions at larger scales. The main physiographic boundaries occur where the fault trace splits into two parallel splays at Green Canyon and at Blacksmith Fork (for example at section boundaries). The northern and southern sections display two range fronts, a western, lower-relief (200-500 m; 656-1,640 ft) sinuous front developed on Tertiary rocks, and an eastern, higher relief (900 m; 2,952 ft) straighter front cut in Paleozoic rocks. The central section has only a single steep 900-meter-high (2,952 ft) front cut in Paleozoic rocks (figure 17). Two aspects of range-front morphology, faceted-spur structure and drainage-basin morphology, yield quantitative comparisons among the three physiographic sections.

Faceted Spurs

Previous workers (Wallace, 1978; Bull, 1984) have presented conceptual models of how faceted range fronts can preserve elements of tectonic history. On the Wasatch fault zone, Hamblin and Best (1978) and Anderson (1977) mapped individual sets of facets above the fault and deduced that long-term periods of tectonic uplift had alternated with periods of quiescence and pedimentation. On the ECFZ, the objective of faceted spur study was less oriented to chronology (due to the inability to date facet sets) than to a comparison of facet geometry between the three physiographic sections of the ECFZ. Distinct differences in the number of and elevation of facet sets between the sections would suggest that they are tectonically persistent seismogenic segments. Conversely, if facet trends are traceable across section boundaries, it would appear that sections defined by orientation, and even by late Quaternary fault scarps, may not be representative of the entire Neogene period.

Methods

Facets were distinguished on 1:24,000 topographic maps by tracing bounding ridge lines upslope until they merged at a facet crest. All ridge lines that intersect the ECFZ were traced in this manner along the 56 kilometer (34 mi) length of the Bear River Range front in Utah. If no intervening, isolated summits occur, these facets can extend all the way to the range crest at elevations up to 2,865 meters (9,397 ft). From the 1:24,000 maps, the facets were transferred to a vertical-plane projection that mimics a distant, "telescoped" view of the range front. This projection is shown in figure 18, where the vertical exaggeration is 4 times.

Correlating sets of facets is a difficult task, and no standardized technique has been widely adopted. Menges (1988) and Zuchiewicz and McCalpin (1992) ranked range-front facets by order. Orders were assigned by applying the stream network ordering systems of Shreve (1966) and Horton (1945), respectively, to the network of interfluvies on each facet. However, sometimes adjacent facets of similar size and height would fall into different orders due to variations in interfluvie density and branching structure, often reflecting variable bedrock lithology and structure (Zuchiewicz and McCalpin, 1992). Therefore, facets on the Bear River Range front were correlated primarily on the elevation of facets crests, after the method of Anderson (1977).

The method employed was to start along-strike facet correlations by connecting the crest elevations of the lowest set of well-defined facets (level 1 on figure 18). These facets are the youngest, steepest, least dissected, and most numerous, all of which give some confidence in lateral correlation. The general degree of facet erosion and incision helps to identify higher facets of similar age, but crest elevations seem to have more deviation within higher sets than within the lower facet sets. Correlating facet sets higher than the lowest two or three sets becomes somewhat subjective. Unfortunately, one's correlation of facet crests tends to be influenced by previous (lower) facet correlation lines, such that higher correlation lines are usually drawn parallel to lower lines. This method results in a conservative, simple interpretation. Almost by definition, the method eliminates the possibility of highly diverging or converging facet correlation lines, although they could conceivably exist in nature. Accordingly, limited confidence can be placed in the detailed interpretation of upper facet data.

Results

The central fault section exhibits the best faceted spurs. Between Green Canyon and Blacksmith Fork, six facet crest levels can be continuously traced and a seventh level is less well preserved (figures 17 and 18). Because the base of the range front is nearly horizontal (at elevation 1,585 m; 5,200 ft), the two lowest facet correlation lines are roughly horizontal. All successive facet sets seem to gain elevation as traced from north to south, from set 3 (60 m; 200 ft gain), to set 4 (120 m; 400 ft gain), to set 5 (180 m; 600 ft gain), to set 6 (120 m; 400 ft gain), to set 7 (240 m; 800 ft gain). This apparent northward tilt ranges from 0.22° in lower facets to 0.9° in upper facets. The tilt could be due to: (1) incorrect correlation, especially across Logan, Providence, or Millville Canyons, or (2) a long-term, progressive

northward tilt of the upthrown block of the central section. The progressive increase of tilts in older facet sets suggests the trend is real, and not an artifact of the method.

Surprisingly, similar facet sets are found north of Green Canyon in the southern part of the northern section. The base of the range front cut on Paleozoic rocks rises steeply to the north, uplifted by fault movement on the western splay, which itself has a poorly developed range front cut on Tertiary rocks (not shown on figure 18). The definition of the five facet sets decreases to the north; north of Dry Canyon, only four, widely spaced facets can be found. The small, steep, undissected facets are missing north of Dry Canyon, suggesting that little late Neogene fault movement has occurred on this eastern splay of the fault. This interpretation agrees with previously discussed observations of more recent movement on the western fault splay in the northern section.

The southern part of the northern section is anomalous; it appears to be a steeply south-tilted extension of the central section. If correct, this interpretation implies that the central section may have previously extended to Dry Canyon. After formation of the lowest facet set (late in the Neogene) this northern part of the central section (north of Green Canyon) was presumably uplifted and tilted southward by a shift of movement to the western splay fault. This sense of relative movement between the northern and central sections (northern

section facets higher than central section facets) is itself anomalous. One would expect the central section footwall block to be higher than that of the northern block, because range-front morphology indicates the central section is more tectonically active than its flanking sections. However, shoreline elevations suggest that during the latest two faulting events, the central segment footwall remained nearly stationary, with most relative displacement occurring as hanging-wall subsidence. The facet evidence suggests that, during Neogene time, faulting events on the central segment may have resulted in absolute (geodetic) subsidence of both the upthrown and downthrown blocks, leading to the anomalously low position of the central segment footwall block relative to the northern and southern blocks.

The southern section facets are likewise tilted down toward the central section. The lower three facet sets in the southern section seem to match central section sets well, with the correlation more speculative at higher levels. The lowest, youngest facet set is similar in height and morphology to the lowest set in the central section. This geometry implies that late Neogene faulting in the southern section has occurred on the eastern splay, rather than shifting to the western one, as occurs on the northern section. Supporting this conclusion is the presence of pre-Bonneville fault scarps on the eastern splay of the southern section, and their absence on the western splay.



Figure 17. Photograph of faceted spurs along the Bear River Range front, in the central segment of the ECFZ; view is to the east. Logan Peak (elevation 2,960 m [9,170 ft]) is the highest summit at upper left; Providence, Utah (elevation 1,402 m [4,600 ft]) is at bottom center. Hell's Kitchen (marked "HK" at the range front) marks the southernmost limit of continuous post-Bonneville fault scarps in the central segment.

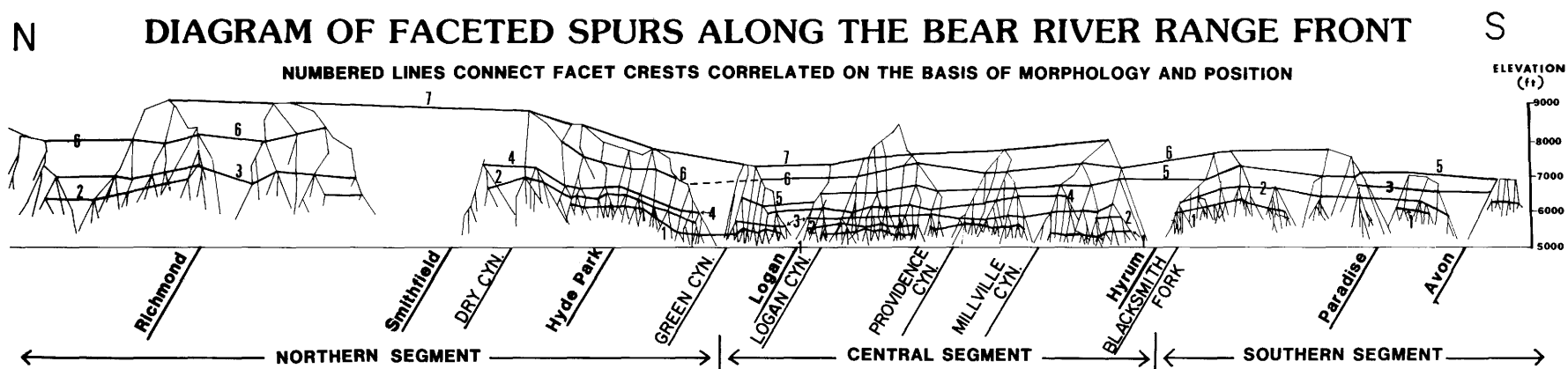


Figure 18. Diagram of faceted spurs along the Bear River Range front. Thin lines connect the crests of individual facets cut on Paleozoic rocks on the eastern splays of the northern and southern (geometric) fault segments, and on the central (seismogenic) segments. Heavy numbered lines connect facet crests correlated on the basis of morphology and position; 1 is the youngest facet set, 7 is the oldest. Range front structure on the western splay faults, cut on softer Tertiary rocks, is not shown. Facets in the northern and southern (geometric) segments are higher than correlative facets in the central segment, probably due to range front uplift by the western splay faults in the end segments. Town names are in lower case letters, canyon names are in upper case letters.

In summary, my interpretation of facet structure indicates that relative movement on the splays of the ECFZ is not identical on the northern and southern sections. On the northern section, the western splay fault exhibits younger movement than the eastern splay. Late Neogene (but pre-Bonneville) events extended from the central section northward to Dry Canyon on the eastern splay, but in later Neogene time rupture has been diverted to the western splay. At the southern end of the fault, in contrast, the western splay fault developed earlier in early (?) Neogene time. After some activity and relative movement on the western splay, middle(?) to late Neogene events have occurred persistently on the eastern splay. Many of these pre-Bonneville events may have included simultaneous uplift on the central section, indicating that, in a long-term sense, the proposed segment boundary at Blacksmith Fork is probably not persistent.

Drainage Basin Analysis

The tectonic geomorphology of a fault-generated range front is reflected by drainage basin morphology as well as by faceted spur structure. Wallace (1978) suggested that more active range fronts would contain more elongate drainage basins in their mountain blocks. Steepest stream gradients would be found closer to the range front, where valleys would be narrowest. MacLean (1986) used 10 morphometric parameters to characterize sections of the Wasatch fault. These parameters were: (1) mountain front sinuosity, (2) drainage basin shape, (3) stream length, (4) stream relief, (5) valley morphology, (6) slope uniformity, and (7-10) four measurements relating to maximum stream gradient.

A slightly different approach was used in this study. Mountain front sinuosity is difficult to measure objectively (depending on map scale and assumptions), and may be a relatively insensitive parameter for small differences in slip rate, so this parameter was omitted from this study. Basin shape (a dimensionless ratio of basin area to the area of a circular basin with the same maximum diameter) was used, with the assumption that more elongate basins represented more active sections. Stream length and basin area were measured, because less active range fronts tend to have longer and larger drainage basins, lacking the many short small basins coming from small, steep faceted spurs of recent origin. MacLean (1986) analyzed only basins with lengths between 2,743 and 12,195 meters (9,000 and 40,000 ft). By concentrating on large basins, she overlooked most basins developed on the faceted spurs themselves, which are rarely longer than 2,440 meters (8,000 ft). However, most tectonic information may reside in the structure of tectonically generated basins on the range front itself (figure 17), and not in larger basins that may be strongly influenced by bedrock stratigraphy and structure within the upthrown block.

In this study, every mappable drainage line that crossed the ECFZ was identified and measured. A total of 66 basins were analyzed for their gross structure (29 in the northern section, 22 in the central section, 15 in the southern section). In each basin three parameters were measured: (1) basin shape, (2) basin area,

and (3) basin length. Histograms of basin shapes in the three sections are presented in figure 19a. In each section the distribution of shapes is roughly normal (from the X^2 test) with mean shape factors ranging from 0.23 (very elongate) to 0.37 (moderately elongate). A perfectly circular basin would yield 1.0. Comparison of the mean values by the ANOVA Table (Minitab statistical package) indicates the means are different at the 5 percent confidence level. If Wallace's (1978) model is correct, the more elongate basins should be found in the more active fault segments. Based on geomorphic and stratigraphic evidence discussed earlier, this order would be central section (most elongate), northern section (due to steep basins in its southern third) and southern section (least elongate). The observed order of basin shape factors is identical; 0.23 in the central section (considerably more elongate than the other two), 0.36 in the northern and 0.37 in the southern sections. The shape/frequency distribution is also different between the central section and the other two sections. In the central section the median shape class is the most elongate class, reflecting an abundance of linear basins developed on steep, dissected facets. In the northern and southern sections, more rounded basins predominate, indicating that tributaries are extending headward at other than right angles to the range front. This better-integrated pattern suggests weaker tectonic influence and a lower uplift rate in the end sections.

Basin area was examined because casual observation showed many more small basins on recent facets in the central section, as opposed to end sections. The basin area/frequency distributions in each section are exponential (figure 19b). Between 76 percent and 82 percent of all basins are in the smallest area class (0-5 km²; 0-2 mi²), yet basins up to 41 km² (16 mi²) are present. Comparison of mean values shows that the smallest basins are found on the southern section, not on the central section as predicted by Wallace's model. However, the frontal mountain ridge in the southern section is smaller than in the other two sections; thus basins are limited in size, even if they reach the ridge crest. Because no large basins can occur, the frequency distribution is truncated on the large side, which reduces the mean values and standard deviation for the southern section. In the northern and central sections, where facets rise to similar heights, the central section has smaller basins (figure 19b).

Stream length was measured to compute basin shape. According to the conceptual model, more active range fronts should contain more abundant short basins on small facets. Within each section of the ECFZ the basin length/frequency distribution is exponential, indicating a predominance of shorter basins (figure 19c). The shortest basins are found in the southern section, followed by the northern, and then central sections. The shorter basins of the southern section can be explained by the smaller size of the frontal ridge. The central section has the longest basins, which may indicate that its facets are larger and higher than those in the northern section.

In summary, basin shapes are more elongate in the central section than in the two end sections, but basin area and length in the central section do not correspondingly indicate more active tectonism. Factors other than tectonics may be influencing basin morphometry, such as the variable stratigraphy exposed in range-front basins. The axis of the north-northeast-

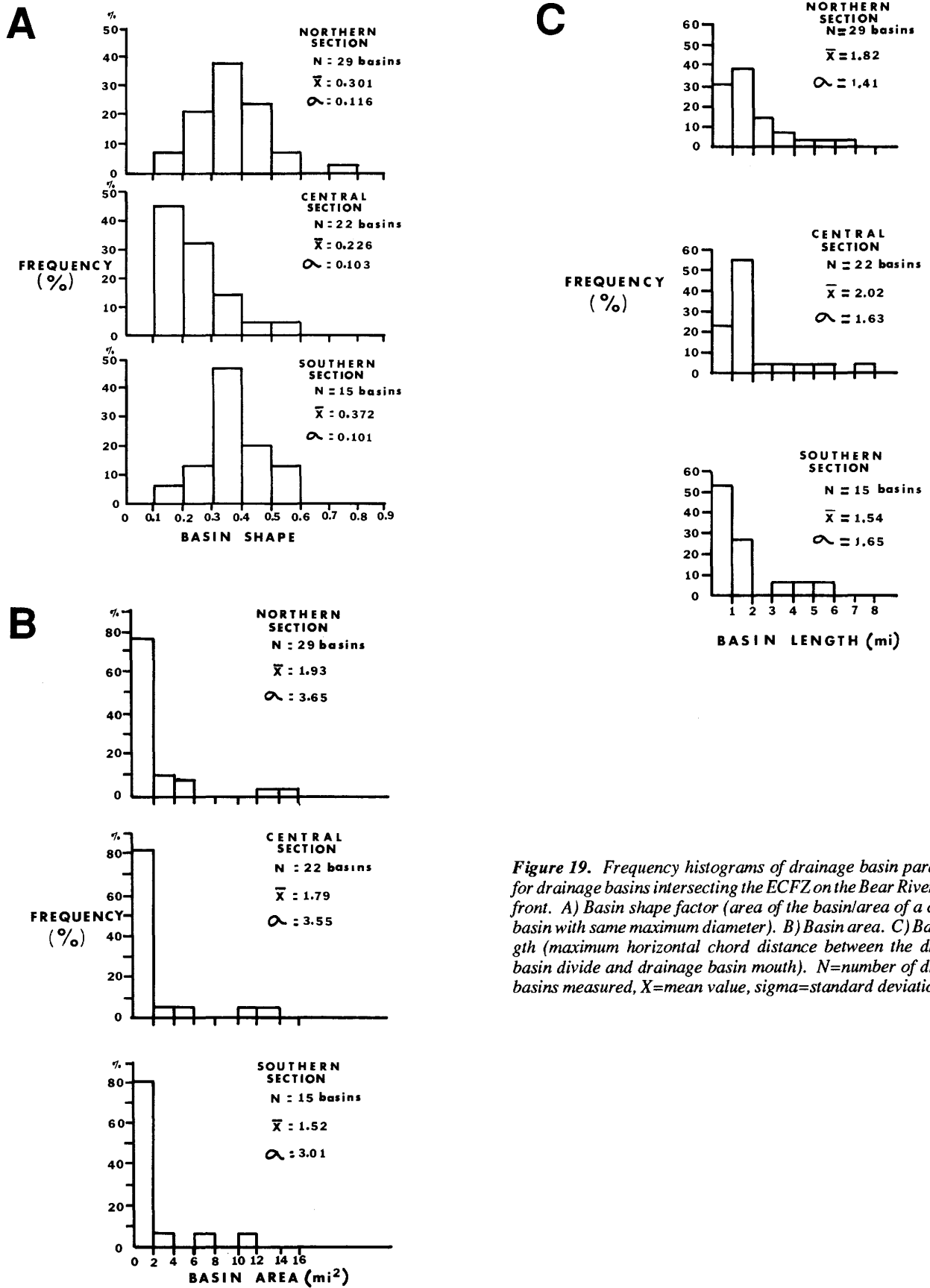


Figure 19. Frequency histograms of drainage basin parameters for drainage basins intersecting the ECFZ on the Bear River Range front. A) Basin shape factor (area of the basin/area of a circular basin with same maximum diameter). B) Basin area. C) Basin length (maximum horizontal chord distance between the drainage basin divide and drainage basin mouth). N=number of drainage basins measured, X=mean value, sigma=standard deviation.

trending Logan Peak syncline (Williams, 1948) converges with the range front southward, bringing progressively younger rocks to the range front from north to south. Basins of the northern section are predominantly in Precambrian quartzites, while in the central section Ordovician to Devonian carbonates dominate, and in the southern section Devonian to Pennsylvanian clastics are most abundant.

CONCLUSIONS

The Quaternary history of the ECFZ can be deduced by the relation of fault scarps to Quaternary deposits, by deformation of the Bonneville-highstand shoreline, and by tectonic geomorphology of the range front. Three fault sections are suggested by gross structural geology, physiography, and presence of post-Bonneville fault scarps. In the northern and southern sections (26 km or 16 mi and 14 km or 8.4 mi long, respectively), the fault zone includes several parallel, north-trending splays roughly 2 kilometers (1.2 mi) apart. Two range fronts occur in these end sections, a subdued western one cut onto Tertiary rocks, and a steeper eastern one cut onto Proterozoic and Paleozoic rocks. Bonneville and younger sediments are usually not faulted in end sections, although in places Bonneville sediments contain structures possibly related to lateral spreading or landsliding. In contrast, the central section (16 km; 9.6 mi long) contains a single fault trace at the base of a straight, steep range front cut onto Paleozoic rocks. This section is probably also a seismogenic segment. Two post-Bonneville-highstand, surface-faulting events have created composite fault scarps with up to 4.2 meters (13.8 ft) surface offset over a distance of at least 8 kilometers (4.8 mi). Radiocarbon and TL age estimates from two trenches across fault scarps indicate that an earlier event, with 1.4 to 1.9 meters (2.6-6.2 ft) displacement, occurred between 13 and 15.5 thousand years ago. A second event occurred about 4 thousand years ago with 0.5 to 1.2 meters (1.6-3.9 ft) of displacement. Inferred magnitudes for these two paleoearthquakes range from M_s 6.6 to 7.1.

The Bonneville highstand shoreline has been deformed by regional and local factors along the ECFZ subsequent to its formation about 15 thousand years ago. However, the local vertical shoreline anomalies do not correlate with either the extent of post-Bonneville fault scarps or with inferred fault segment boundaries. Instead, broad downwarps appear superimposed on regional isostatic rebound only at locations of major deltas of the Bonneville lake cycle. Rheologic modeling of the crust as a beam subjected to point depositional loading indicates that downwarps may have been caused by the rapid loading of deltaic material on the downthrown block of the ECFZ.

The tectonic geomorphology of the range front indicates that segments defined by post-Bonneville faulting have not been persistent throughout the late Cenozoic. Faceted spur structure implies that the northern/central section boundary may have shifted several kilometers southward in late Neogene time, probably associated with late development of the western splay fault of the northern section. On the southern section, in contrast, the western splay developed earlier than the eastern one, and late Neogene uplift has largely abandoned the western splay for

movement on the eastern splay. Young spur structure on the central and southern sections is very similar, implying that some late Neogene ruptures may have spanned both sections (>29 km; >17 mi long).

Earthquake potential can be assessed by comparing average recurrence interval with time since latest faulting. The recurrence interval between the two latest events has a mean value of 10.3 thousand years. Evidence for an even earlier displacement event between 15.5 thousand and 19.5 thousand years ago is equivocal; if it occurred, recurrence time between it and the dated penultimate event is less than 4 thousand years. In contrast, the elapsed time since latest event is 4 thousand years. Thus, the elapsed time is within the range of estimated recurrence intervals. However, both the penultimate event (13-15.5 thousand years ago) and the inferred earlier event may have been influenced by Lake Bonneville water loading and induced stresses, such that the earlier recurrence times may have been shorter than those to be expected in non-pluvial (modern) climates.

ACKNOWLEDGMENTS

Numerous individuals contributed advice and labor to this project. Michael Machette, Steve Personius, and Alan Nelson (U.S. Geological Survey, Denver) discussed the subdivision of map units and made available copies of their unpublished compilations of Wasatch Front surficial geology. Nelson also loaned the author aerial photographs of the ECFZ. Mike Lowe (UGS; formerly Weber County Planning Commission, Ogden, Utah) allowed use of his unpublished surficial geologic mapping in the Smithfield quadrangle. David Schwartz (U.S. Geological Survey, Menlo Park) provided unpublished photographs of test pits dug by Woodward-Clyde Consultants south of Green Canyon. Gayle McCaLpin assisted in scarp profiling and many manual excavations. The Geology 630 class at Utah State University logged the canal landslide exposure south of the Utah State University campus. Clyde Hardy (Utah State University) first showed that exposure to the author.

Logging at the Bonneville trench was performed by Michael Jackson and Margaret Berry (University of Colorado, Boulder) and by John Garr and John Rice (Utah State University). L.C. Allen Jones (Utah State University) helped log the Provo trench. Permission to trench at the Bonneville and Provo sites was kindly provided by landowner Carol Smith of Logan and the Board of Directors of the Logan Golf and Country Club, respectively. Trench shoring was provided by Dennis Williams (U.S. Bureau of Reclamation, Provo, Utah). The Provo trench was excavated and backfilled by Mr. Steve Kyriopolis, Director of the Parks and Recreation Department, City of Logan, and by Mr. John Pappas, Assistant Director, Utah State University Physical Plant Department. Mr. Randy Oldham, Superintendent of the Logan Country Club golf course, provided invaluable assistance.

Shoreline surveying was directed by Jeff Henkelman, assisted by Thor Dyson, David Fulton, and John Cooper (all of Utah State University). Thermoluminescence dating and laboratory data were provided by Jerry Stipp and Darden Hood (Alpha Analytic Inc., Coral Gables, Florida) with additional dose rate and age interpretation by Steven Forman (INSTAAR,

University of Colorado, Boulder). Richard DeVan (Utah State University) performed the drainage basin analysis, and James Evans (also of Utah State University) provided the rheologic beam model of shoreline deformation. This manuscript bene-

fitted from critical reviews by Stephen F. Personius and Michael W. West. Funding for preparation of this report was provided by the Utah Geological Survey Mineral Lease Special Projects Program.

REFERENCES

- Adamson, R.D., Hardy, C.T., and Williams, J.S., 1955, Tertiary rocks of Cache Valley, Utah and Idaho: Utah Geological Society, Guidebook No. 10, p. 1-22.
- Anderson, T.C., 1977, Compound faceted spurs and recurrent movement in the Wasatch fault zone, north-central Utah: Brigham Young University Studies in Geology, v. 24, no. 2, p. 83-101.
- Arabasz, W.J., Richins, W.D., and Langer, C.J., 1979, The Idaho-Utah border (Pocatello Valley) earthquake sequence of March-April, 1975, in Arabasz, W.J. and others, editors, Earthquake studies in Utah, 1850 to 1979: Salt Lake City, University of Utah Seismograph Stations, Special Publication, p. 339-374.
- Bailey, R.W., 1927, The Bear River Range fault, Utah: American Journal of Science, 5th ser., v. 13, p. 497-502.
- Birkeland, P.W., Berry, M.E., and Swanson, D.K., 1991, Use of soil catena field data for estimating relative ages of moraines: Geology, v. 19, no. 3, p. 281-283.
- Bonilla, M.G., Mark, R.K., and Lienkaemper, J.J., 1984, Statistical relations among earthquake magnitude, surface rupture length, and surface fault displacement: Bulletin of the Seismological Society of America, v. 74, p. 2379-2411.
- Bradley, W.C., and Griggs, G.B., 1976, Form, genesis, and deformation of central California wave-cut platforms: Geological Society of America Bulletin, v. 87, no. 3, p. 433-449.
- Brummer, J.E., 1990, Origin of low-angle normal faults along the western side of the Bear River Range in northern Utah: Logan, Utah State University, unpublished M.S. thesis, 121 p.
- Brummer, J.E., and McCalpin, J.P., 1990, Geologic map of the Richmond quadrangle, Cache County, Utah: Utah Geological and Mineral Survey, Open-File Report 174, 45 p., scale 1:24,000.
- Bucknam, R.C., and Anderson, R.E., 1979, Estimation of fault scarp ages from a scarp-height-slope-angle relationship: Geology, v. 7, p. 11-14.
- Bull, W.B., 1984, Tectonic geomorphology: Journal of Geological Education, v. 32, p. 310-324.
- Cluff, L.S., Glass, C.E., and Brogan, G.E., 1974, Investigation and evaluation of the Wasatch fault north of Brigham City, and Cache Valley faults, Utah and Idaho: Woodward-Lundgren and Associates, unpublished report to the Utah Geological and Mineral Survey, 147 p.
- Crittenden, M.D., Jr., 1963, New data on the isostatic deformation of Lake Bonneville: U.S. Geological Survey Professional Paper 454-E, 31 p.
- Currey, D.R., and Oviatt, C.G., 1985, Durations, average rates, and probable causes of Lake Bonneville expansions, stillstands, and contractions during the last deep-lake cycle, 32,000 to 10,000 years ago, in Kay, P.A. and Diaz, H.F., editors, Problems of and prospects for predicting Great Salt Lake levels: Salt Lake City, University of Utah, Center for Public Affairs and Administration, p. 9-24.
- dePolo, C.M., Clark, D.G., Slemmons, D.B., and Ramelli, A.R., 1991, Historical surface faulting in the Basin and Range Province, western North America — Implications for fault segmentation: Journal of Structural Geology, v. 13, no. 2, p. 123-136.
- Evans, J.P., 1991, Structural setting of seismicity in northern Utah: Utah Geological Survey, Contract Report 91-15, 37 p., 4 plates, scale 1:100,000.
- Evans, J.P., McCalpin, J.P., and Holmes, D.C., 1991, Geologic map of the Logan quadrangle, Cache County, Utah: Utah Geological Survey Open-File Report 229, 59 p., 2 plates, scale 1:24,000.
- Evans, J.P., and Oaks, R.Q., 1990, Geometry of horizontal extension in the northeastern Basin and Range superimposed on the Sevier fold and thrust belt [abs.]: Geological Society of America Abstracts with Programs, v. 22, no. 6, p. 10.
- Forman, S.L., 1989, Application and limitations of thermoluminescence to date Quaternary sediments: Quaternary International, v. 1, p. 47-59.
- Forman, S.L., Wintle, A.G., Thordarson, H.L., and Wyatt, P.H., 1987, Thermoluminescence properties and age estimates of Quaternary marine sediments from the Hudson Bay lowland, Canada: Canadian Journal of Earth Sciences, v. 24, p. 2405-2411.
- Fuller, M.L., 1912, The New Madrid earthquake: U.S. Geological Survey Bulletin 494, 112 p.
- Galloway, C.L., 1970, Structural geology of the eastern part of the Smithfield quadrangle, Utah: Logan, Utah State University, unpublished M.S. thesis, 115 p.
- Gilbert, G.K., 1890, Lake Bonneville: U.S. Geological Survey Monograph 1, 435 p.
- Gile, L.H., Peterson, F.F., and Grossman, R.B., 1966, Morphological and genetic sequences of carbonate accumulation in desert soils: Soil Science, v. 101, p. 347-360.
- Hamblin, W.K., and Best, M.G., 1978, Patterns and rates of recurrent movement along the Wasatch-Hurricane-Sevier fault zone, Utah, during late Cenozoic time: U.S. Geological Survey, Earthquake Hazards Reduction Program Summaries of Technical Reports, v. 5, p. 70-71.
- Hancock, P.L., Yeats, R.S., and Sanderson, D.J., special editors, 1991, Characteristics of active faults (special issue): Journal of Structural Geology, v. 13, no. 2, 240 p.
- Hanks, T.C., and Kanamori, Haroo, 1979, A moment magnitude scale: Journal of Geophysical Research, v. 84, p. 2981-2987.
- Hetenyi, M., 1946, Beams on elastic foundations: Ann Arbor, University of Michigan Press, 255 p.
- Horton, R.E., 1945, Erosional development of streams and their drainage basins: Geological Society of America Bulletin, v. 56, p. 275-370.
- Johnson, A.M., 1970, Physical processes in geology: San Francisco, Freeman, Cooper, and Co., 577 p.
- Keaton, J.R., 1987, Potential consequences of earthquake-induced regional deformation along the Wasatch Front, north-central Utah, in McCalpin, James, editor, Proceedings of the 23rd Symposium on Engineering Geology and Soils Engineering: Logan, Utah State University, p. 19-34.

- Khromovskikh, V.S., 1989, Determination of magnitudes of ancient earthquakes from dimensions of observed seismodislocations: *Tectonophysics*, v. 166, p. 1-12.
- Lowe, M.V., 1987, Surficial geology of the Smithfield quadrangle, Cache County, Utah: Logan, Utah State University, unpublished M.S. thesis, 143 p.
- Lowe, Mike, and Galloway, C.L., 1993 Provisional geologic map of the Smithfield quadrangle, Cache County, Utah: Utah Geological Survey Map 143, 18 p., 2 pl., 1:24,000.
- Mabey, D.R., 1985, Geophysical maps of the Mount Naomi Roadless Area, Cache County, Utah and Franklin County, Idaho: U.S. Geological Survey Miscellaneous Field Investigations Map MF-1566-C, scale 1:100,000.
- Machette, M.N., Personius, S.F., and Nelson, A.R., 1987, Quaternary geology along the Wasatch fault zone — Segmentation, recent investigations, and preliminary conclusions, *in* Gori, P.L., and Hays, W.W., editors, Evaluation of urban and regional earthquake hazard and risk in Utah: U.S. Geological Survey Open-File Report 87-585, p. A1-A72.
- Machette, M.N., Personius, S.F., and Nelson, A.R., 1992, Paleoseismology of the Wasatch fault zone — A summary of recent investigations, interpretations, and conclusions, *in* Gori, P.L., and Hays, W.W., editors, Assessment of regional earthquake hazard and risk along the Wasatch Front, Utah: U.S. Geological Survey Professional Paper 1500-A, p. A1-A71.
- Machette, M.N., Personius, S.F., Nelson, A.R., Schwartz, D.P., and Lund, W.R., 1991, The Wasatch fault zone, Utah — Segmentation and history of Holocene earthquakes: *Journal of Structural Geology*, v. 13, no. 2, p. 137-150.
- Machette, M.N., and Scott, W.E., 1988, A brief review of research on lake cycles and neotectonics of the eastern Basin and Range Province, *in* Machette, M.N., editor, *In the footsteps of G.K. Gilbert — Lake Bonneville and neotectonics of the eastern Basin and Range Province*: Utah Geological and Mineral Survey Miscellaneous Publication 88-1, p. 7-16.
- MacLean, Alison, 1985, Quaternary segmentation of the Wasatch fault zone, Utah, as studied by morphometric discriminant analysis: Miami, Ohio, Miami University, unpublished M.S. thesis, 200 p.
- McCalpin, James, 1987a, Late Quaternary faulting and earthquake hazard in Cache Valley, Utah: Unpublished Final Technical Report to U.S. Geological Survey, contract no. 14-08-0001-G1091, 187 p.
- McCalpin, James, 1987b, Geologic criteria for recognition of individual paleoseismic events in extensional environments, *in* Crone, A.J. and Omdahl, E.M., editors, *Directions in Paleoseismology*, Proceedings of Conference XXXIX: U.S. Geological Survey Open-File Report 87-673, p. 102-114.
- McCalpin, James, 1988, The history of Lake Bonneville in Cache Valley, Utah — Updating Gilbert's observations, *in* Machette, M.N., editor, *In the footsteps of G.K. Gilbert — Lake Bonneville and neotectonics of the eastern Basin and Range Province*: Utah Geological and Mineral Survey Miscellaneous Publication 88-1, p. 111-116.
- McCalpin, James, 1989, Surficial geologic map of the East Cache fault zone, Cache County, Utah: U.S. Geological Survey Miscellaneous Field Investigations Map MF-2107, scale 1:50,000.
- McCalpin, James, and Garr, J.D., 1984, Pleistocene lake shorelines in Pocatello Valley, Idaho and Utah, and their uses in neotectonic reconstruction [abs.]: *Geological Society of America Abstracts with Programs*, v. 16, no. 4, p. 247.
- McCalpin, James, and Forman, S.L., 1991, Late Quaternary faulting and thermoluminescence dating of the East Cache fault zone, north-central Utah: *Bulletin of the Seismological Society of America*, v. 81, no. 1, p. 139-161.
- McCalpin, James, Robison, R.M., and Garr, J.D., 1987, Neotectonics of the Hansel Valley-Pocatello Valley corridor, northern Utah and southern Idaho, *in* Gori, P.L. and Hays, W.W., editors, *Evaluation of urban and regional earthquake hazard and risk in Utah*: U.S. Geological Survey Open-File Report 87-585, p. G1-G39.
- McCalpin, James, Robison, R.M., and Garr, J.D., 1992, Neotectonics of the Hansel Valley - Pocatello Valley corridor, northern Utah and southern Idaho, *in* Gori, P.L. and Hays, W.W., editors, *Assessment of regional earthquake hazard and risk along the Wasatch Front*, Utah: U.S. Geological Survey Professional Paper 1500-G, p. G1-G18.
- Mendenhall, A.J., 1975, Structural geology of eastern part of Richmond and western part of Naomi Peak quadrangles, Utah-Idaho; Logan, Utah State University, unpublished M.S. thesis, 45 p.
- Menges, C.M., 1988, The tectonic geomorphology of mountain front landforms in the northern Rio Grande rift of New Mexico: Albuquerque, University of New Mexico, unpublished Ph.D. dissertation, 339 p.
- Mullens, T.E., and Izett, G.A., 1964, Geology of the Paradise quadrangle, Cache County, Utah: U.S. Geological Survey Bulletin 1181-5, 32 p.
- Myers, W.B., and Hamilton, Warren, 1964, Deformation accompanying the Hebgen Lake earthquake of August 17, 1959: U.S. Geological Survey Professional Paper 435, p. 55-98.
- Nelson, A.R., 1987, A facies model of colluvial sedimentation adjacent to a single-event normal-fault scarp, Basin and Range Province, western United States, *in* Crone, A.J., and Omdahl, E.M., editors, *Directions in Paleoseismology — Proceedings of Conference XXXIX*: U.S. Geological Survey Open-File Report 87-673, p. 136-145.
- Nelson, A.R., 1988, The northern part of the Weber section of the Wasatch fault zone near Ogden, Utah, *in* Machette, M.N., editor, *In the footsteps of G.K. Gilbert — Lake Bonneville and neotectonics of the eastern Basin and Range Province*: Utah Geological and Mineral Survey Miscellaneous Publication 88-1, p. 33-37.
- Nelson, A.R., 1992, Lithofacies analysis of colluvial sediments — An aid in interpreting the recent history of Quaternary normal faults in the Basin and Range Province, western United States: *Journal of Sedimentary Petrology*, v. 62, p. 607-621.
- Nelson, A.R., and Sullivan, J.T., 1987, Late Quaternary history of the James Peak fault, southernmost Cache Valley, north-central Utah, *in* Gori, P.L., and Hays, W.W., editors, *Evaluation of urban and regional earthquake hazards and risk in Utah*: U.S. Geological Survey Open-File Report 87-585, p. J1-J39.
- Nelson, A.R., and Sullivan, J.T., 1992, Late Quaternary history of the James Peak fault, southernmost Cache Valley, north-central Utah, *in* Gori, P.L., and Hays, W.W., editors, *Assessment of regional earthquake hazard and risk along the Wasatch Front*, Utah: U.S. Geological Survey Professional Paper 1500-J, p. J1-J13.
- Ostenaar, D.A., 1984, Relationships affecting estimates of surface fault displacements based on scarp-derived colluvial deposits [abs.]: *Geological Society of America Abstracts with Programs*, v. 16, no. 5, p. 327.
- Passy, Q.R., 1981, Upper mantle viscosity derived from the difference in rebound of the Provo and Bonneville shorelines, Lake Bonneville Basin, Utah: *Journal of Geophysical Research*, v. 86, p. 11,701-11,708.
- Personius, S.F., 1988, Preliminary surficial geologic map of the Brigham City segment and adjacent parts of the Weber and Col-

- linston segments, Wasatch fault zone, Box Elder and Weber Counties, Utah: U.S. Geological Survey Miscellaneous Field Studies Map MF-2042, scale 1:50,000.
- Personius, S.F., 1990, Surficial geologic map of the Brigham City segment and adjacent parts of the Weber and Collinston segments, Wasatch fault zone, Box Elder and Weber Counties, Utah: U.S. Geological Survey Miscellaneous Field Investigations Map I-1979, scale 1:50,000.
- Peterson, V.E., 1936, The geology of a part of the Bear River Range and some relationships that it bears with the rest of the range: Logan, Utah State University, unpublished M.S. thesis, 71 p.
- Rendell, H.M., and Townsend, P.D., 1988, Thermoluminescence dating of a 10 meter loess profile in Pakistan: *Quaternary Science Reviews*, v. 7, p. 251-255.
- Rogers, J.L., 1978, Geologic reconnaissance of a portion of the Logan east bench: Utah Geological and Mineral Survey unpublished technical memorandum, 51 p.
- Rose, J., 1981, Raised shorelines, in Goudie, Andrew, editor, *Geomorphological techniques*: London, Allen and Unwin, p. 327-341.
- Schwartz, D.P., and Sibson, R.H., editors, 1989, Fault segmentation and controls of rupture initiation and termination: U.S. Geological Survey Open-File Report 89-315, 447 p.
- Scott, W.E., McCoy, W.D., Shroba, R.R., and Rubin, Meyer, 1983, Reinterpretation of the exposed record of the last two lake cycles of Lake Bonneville, western United States: *Quaternary Research*, v. 20, no. 3, p. 261-285.
- Shannon and Wilson and Agbabian Associates, 1980, Geotechnical data from accelerograph stations investigated during the period 1975-1979: U.S. Nuclear Regulatory Commission Summary Report NUREG/CR 1643.
- Shreve, R.L., 1966, Statistical law of stream numbers: *Journal of Geology*, v. 74, p. 17-37.
- Shroba, R.R., 1980, Influence of parent material, climate, and time on soils formed on Bonneville shoreline and younger deposits near Salt Lake City and Ogden, Utah [abs.]: *Geological Society of America Abstracts with Programs*, v. 12, no. 6, p. 304.
- Shroba, R.R., 1987, Variation in clay content and morphological development of soil argillic B horizons in deposits of latest Pleistocene age, Colorado and Utah [abs.]: *Geological Society of America Abstracts with Programs*, v. 19, no. 5, p. 334.
- Slemmons, D.B., 1982, Determination of design earthquake magnitudes for microzonation: Third International Earthquake Microzonation Conference Proceedings, v. 1, p. 119-130.
- Smith, R.B., and Bruhn, R.L., 1984, Intraplate extensional tectonics of the eastern Basin-Range; inferences on structural style from seismic reflection data, regional tectonics, and thermal-mechanical models of brittle-ductile deformation: *Journal of Geophysical Research*, v. 89, no. B7, p. 5733-5762.
- Stein, R.S., and Barrientos, S.E., 1985, Planar high-angle faulting in the Basin and Range — Geodetic analysis of the 1983 Borah Peak, Idaho, earthquake: *Journal of Geophysical Research*, v. 90, no. B 13, p. 11,355-11,366.
- Swan, F.H., III, Hanson, K.L., Schwartz, D.P., and Black, J.H., 1983, Study of earthquake recurrence intervals on the Wasatch fault, Utah: Unpublished Eighth Semi-Annual Technical Report, May 1983, U.S. Geological Survey contract no. 14-08-0001-19842, 20 p.
- Wallace, R.E., 1978, Geometry and rates of change of fault-generated range fronts, north-central Nevada: U.S. Geological Survey, *Journal of Research*, v. 6, no. 5, p. 637-650.
- Westaway, R. and Smith, R.B., 1989, Source parameters of the Cache Valley (Logan), Utah, earthquake of 30 August 1962: *Bulletin of the Seismological Society of America*, v. 79, p. 1410-1425.
- Wheeler, R.L., 1989, Persistent segment boundaries on basin-range normal faults, in Schwartz, D.P., and Sibson, R.H., editors, *Fault segmentation and controls of rupture initiation and termination*: U.S. Geological Survey Open-File Report 89-315, p. 432-444.
- Wheeler, R.L., and Krystinik, K.B., 1988, Segmentation of the Wasatch fault zone, Utah — Summaries, analysis, and interpretations of geological and geophysical data: U.S. Geological Survey Bulletin 1827, 47 p.
- Williams, J.S., 1948, Geology of the Paleozoic rocks, Logan quadrangle, Utah: *Geological Society of America Bulletin*, v. 59, no. 11, p. 1121-1164.
- Williams, J.S., 1962, Lake Bonneville; Geology of southern Cache Valley, Utah: U.S. Geological Survey Professional Paper 257-C, p. 131-152.
- Wintle, A.G., and Huntley, D.J., 1982, Thermoluminescence dating of sediments: *Quaternary Science Reviews*, v. 1, p. 31-53.
- Zuchiewicz, W., and McCalpin, J.P., 1992, Morphometry of faceted spurs along the north-central Wasatch fault, western U.S.: Stockholm, Sweden, *Bulletin of the INQUA Neotectonics Commission*, no. 15, p. 23-31.

APPENDIX 1 UNIT DESCRIPTIONS FROM THE BONNEVILLE TRENCH

The following descriptions refer to lithologic units differentiated in a 65-meter-long (213 ft) trench across the East Cache fault, Logan, Utah. Trench logging was performed by John Garr, John Rice, and James McCalpin (Utah State University) and Mike Jackson and Margaret Berry (University of Colorado) from October 15 to October 24, 1986. Unit descriptions were made by John Garr and John Rice. Seven major depositional packages are recognized; each package is subdivided into units, consecutively numbered from unit 1 (oldest) to unit 45 (youngest).

PACKAGE 1, LITTORAL SAND

Unit 1- 10YR6/4, predominantly medium sand, though some fine sand and rare coarse sand and pebbles occur; well sorted, well rounded; strongly laminated, laminations 1 centimeter (0.4 in) or less thick, laminations slightly wavy updip, become more regular (flat) downdip; very gentle west dip; numerous CaCO₃-cemented fractures, stringers, laminations, and pods; individual laminations may be slightly cemented.

PACKAGE 2, BEACH GRAVEL, UPTHROWN BLOCK

- Unit 3-** 10YR7/3, fine to medium sand, some coarse sand, pebbles rare; very well sorted; well rounded; some zones well laminated, some zones weakly laminated to massive, laminations generally thin (<1 cm; 0.4 in) and show very gentle west dip; CaCO₃ cementation absent. Some convoluted sand (unit 40) at 16.5 meters (54 ft), and a gravelly sand lens (unit 41) at 18.5 m (61 ft).
- Unit 4-** 10YR6/3, "pea" gravel in a coarse sand matrix; moderately well sorted; well rounded; some minor CaCO₃; basal bed (25 centimeters; 10 in thick) of well-rounded cobbles in a sandy gravel matrix; entire unit moderately well bedded; east dip; "pea" gravel separated from basal cobble bed by 2- to 3-centimeter-thick (1-1.5 in), well-cemented gravel.
- Unit 5-** 10YR7/2, "pea" gravel in sparse coarse sand matrix; well rounded; well sorted; this east-dipping unit is moderately cemented by CaCO₃ and stands in relief; 3 to 5 centimeters (1.2-2 in) thick.
- Unit 6-** 10YR5/2, pebbles in gravelly coarse sand matrix; well rounded; moderately well sorted, occasional cobbles; moderate to well bedded, east dip; beds average 2 to 5 centimeters (0.8-2 in) thick, coarse beds stand in slight relief after weathering/ravelling due to cementation.
- Unit 7-** 10YR7/3, gravels in a medium-coarse sand matrix; well rounded; poorly sorted; this unit (5 to 10 centimeters; 2-4 in thick) stands in slightly greater relief than surrounding beds, probably because it is more matrix rich, also because it is CaCO₃ cemented; east dip.
- Unit 8-** 10YR5/2, gravels in a sparse, coarse-sand matrix, rare cobbles; moderately well sorted; well rounded; moderately well bedded; coarser individual beds (2 to 4 cm; 0.8-1.6 in thick) stand in relief, (some localized areas of weak CaCO₃ cementation particularly in higher portion of unit); east-dipping beds.
- Unit 9-** 10YR7/4, large pebble gravel in a fairly sparse coarse sand and gravel matrix, rare cobbles; well rounded; moderately poorly sorted; unit weakly cemented by CaCO₃, with CaCO₃ accumulation on the base of clasts; poorly to moderately bedded; east dip.
- Unit 10-** 10YR6/4 (matrix) - gravels white due to CaCO₃; basal layer of cobbles in a medium-coarse sandy matrix; 15 to 20 centimeters (6-8 in) thick; poor sorting; cobbles well rounded with thin CaCO₃ coating; CaCO₃ cemented "pea" gravel bed above, matrix medium to coarse sand; gravel moderately well rounded, 15 centimeters (6 in) thick; cobbles imbricated and dipping east.
- Unit 11-** 10YR6/3, small cobbles to gravels (fining upward) in matrix of fine to medium sand; poorly sorted; well rounded; minor CaCO₃ cement; moderately poorly bedded; some imbrication of cobbles (dipping east at low angle).

PACKAGE 3, BEACH GRAVEL, DOWNTHROWN BLOCK

- Unit 12-** 10YR4/4, coarse sand (90%) and gravel (10%); moderately well sorted; subround gravel 0.5 to 3 centimeter (0.2-1.2 in) in diameter; sand is foreset, 7 to 10 degrees downslope; a few CaCO₃ stringers.
- Unit 13-** 10YR4/3, gravelly coarse sand, (small gravel, <0.5 cm; 0.2 in); moderately sorted; horizontal laminations.
- Unit 14-** 10YR5/6, silty fine to medium sand; moderately well sorted; lower contact undulates; forms resistant ledge on wall.
- Unit 15-** 10YR7/3, medium sand, minor coarse sand and very rare floating pebbles; well sorted, cross-bedded.
- Unit 16-** 10YR5/3, gravelly medium to coarse sand; moderately well sorted; well rounded; cross-bedded; some areas show localized weak CaCO₃ cementation; low bulk density; thin 1 to 2 centimeter (0.8 in) laminations; basal "pea" gravel (discontinuous).
- Unit 17-** 10YR6/4, same as unit 43 but clast size is smaller, coarse sand to 1.5 cm (0.6 in) diameter; pebbles matrix is coarser, silt-coarse sand.
- Unit 18-** 10YR6/8, resistant pebbly sand; 95 percent fine to medium sand; pebbles less than 5 percent; up to 2.0 centimeters (0.8 in) in diameter; moderate CaCO₃ accumulation and stringers.
- Unit 19-** 10YR5/4, cross-bedded sandy gravel, occasional "floating" pebbles; CaCO₃ accumulation locally; moderately sorted; sand ranges from medium to coarse grained.
- Unit 20-** 10YR5/4, coarse sand; well sorted; well rounded; well laminated with 1 centimeter (0.4 in) laminations; west dip.
- Unit 21-** 10YR7/6, resistant ledges, similar to unit 44 in upper portion of trench, only free of pebbles.
- Unit 22-** 10YR7/6, silty fine sand; well sorted; moderately well cemented/compacted; west dip.
- Unit 23-** 10YR6/3, coarse sand, occasional floating pebbles; well sorted; well rounded; poorly to moderately laminated, very thin laminations (1 cm; 0.4 in); some areas weakly cemented.
- Unit 24-** 10YR7/3, silty fine to medium sand; well sorted; this unit is discontinuous, similar to unit 26, west dip.
- Unit 25-** 10YR6/3, coarse sand; well sorted; well rounded; moderately well laminated with 1 to 3 centimeters (0.2-1.2 in) thick laminations, laminations disappear near fault zone; some areas weakly cemented by CaCO₃.
- Unit 26-** 10YR7/3, silty fine to medium sand; well sorted; well rounded; unit stands in relief but becomes discontinuous up dip (as it approaches fault); west dip.
- Unit 27-** 10YR6/4, medium to coarse sand; well sorted; well rounded; very similar to unit 29 but not as well laminated up dip and fewer floating pebbles.
- Unit 28-** 10YR7/4, fine to medium sand (some silt); well sorted; well rounded; unit stands in relief and is 1 to 2 centimeters (0.2-0.8 in) thick; west dip.

- Unit 29-** 10YR6/4, medium-coarse sand with “floating” pebbles; well sorted; well rounded; well laminated (laminations to 1-2 cm); west dip.
- Unit 30-** 10YR7/4, fine to medium sand (some silt); well sorted; well rounded; 2 to 4 centimeters (0.8-1.6 in) thick; stands in relief (due to weak CaCO₃ cementation), occasional pods of CaCO₃; west dip.
- Unit 31-** 10YR6/3, coarse sand, occasional pebbles; well sorted; well rounded; some localized pods of CaCO₃ cementation; some thin laminations discernible; grades into unit 29 up dip.
- Unit 32-** 10YR7/3, fine to medium sand (some coarse sand); moderately well sorted; moderately well rounded; moderately to poorly bedded with thin (1 cm; 0.4 in) discontinuous laminations; west dip.
- Unit 33-** 10YR5/4, medium to coarse sand with occasional gravel; moderate to well sorted; well rounded; poorly bedded, but a general fining upward sequence with a discontinuous basal “pea” gravel 4 centimeters (1.6 in) thick.
- Unit 34-** 10YR7/3, “pea” gravel with a sandy matrix; stands in relief due to moderate CaCO₃ cementation; poorly sorted; moderately well rounded; moderately well bedded; west dip.
- Unit 35-** 10YR6/4, gravelly sand; poorly to moderately sorted and rounded; poorly to moderately well bedded, thin (2 cm; 0.8 in) discontinuous beds and laminations; west dip.
- Unit 36-** 10YR7/4, fine to medium sand, some coarse sand and rare floating pebbles, very little silt; moderately well sorted; moderately rounded; some localized pods of CaCO₃-cemented material; fairly massive, very poorly stratified.
- Unit 37-** 10YR6/4, medium to coarse sand (occasional “floating” pebbles); well sorted; moderately well rounded; bedding very difficult to distinguish, massive unstratified sand; load structures and diapirs at lower contact, implies this may be a turbidite.
- Unit 38-** 10YR5/4, fining upward beach gravel; cobbles up to 13 centimeters (5 in) in diameter, subangular to subround, at base; fining to gravel 0.5 to 3 centimeters (0.2-1.2 in) in diameter near top; clast-supported openwork fabric; coarse sand matrix up to 50 percent in upper 25 centimeters (10 in); CaCO₃ coating on undersides of most clasts in lower 30 centimeters (11.8 in); well bedded; 8 to 10 degree west dip.
- Unit 39-** 10YR6/3, medium to coarse sand (80%); poorly sorted; gravel up to 3 centimeters (1.2 in) (20%), subround; a few CaCO₃ coats on larger clasts; very weakly bedded.

PACKAGE 4, DEFORMED BLOCKS/ SAND BLOWS

- Unit 40-** 10YR5/6, same as unit 3.
- Unit 41-** 10YR7/3, gravelly coarse sand, consists of a lens 4 to 8 centimeters (1.6-3.1 in) thick; moderately well sorted; moderately well rounded; some portions weakly cemented by CaCO₃; conformably overlies unit 40; where it grades into the deformed area above faults, this unit has contorted bedding.
- Unit 42-** 10YR7/4, mainly fine to medium sand; well sorted; well rounded; includes undulatory bedding and small diapir structures from 15 to 20 meters (49-66 ft), with increasing deformation toward the main fault plane (25 m; 82 ft); also includes isolated blocks of deformed sand in a massive sand matrix; tectonic faults and fissures from underlying unit 1 die out at the base of this unit; laminated small pods and stringers of CaCO₃; west dip.

PACKAGE 5, GRAVELLY DIAMICTON (DEBRIS FLOW?)

- Unit 43-** 10YR5/4, silty fine to medium sand with pebbles up to 4 centimeters (1.6 in); subround to round; poorly sorted; clasts 70 percent, matrix 30 percent; CaCO₃ coats on undersides of most clasts; clasts generally increase in size downslope, up to 15 centimeters (6 in); mechanical mixture of underlying units (mainly 19, 20, 38, 39) and overlying unit 44.

PACKAGE 6, EOLIAN AND COLLUVIAL SILT

- Unit 44-** 10YR5/6, silty fine to medium sand; moderately well sorted; laminations/bedding not discernible; some zones are moderately well cemented by CaCO₃, these zones seem more sandy; contacts dip very gently to west.

PACKAGE 7, MIXED COLLUVIUM/SLOPEWASH

- Unit 45-** variable colors due to soil formation, silty gravel; poorly sorted; subround to subangular clasts; non-bedded except for rare small concentrations of pebbles; becomes siltier toward top; weak soil formation with no CaCO₃; mantles entire scarp surface.

APPENDIX 2 UNIT DESCRIPTIONS FROM THE PROVO TRENCH

The following descriptions refer to lithologic units differentiated in a 15-meter-long (50 ft) trench across a 1.2-meter-high (4 ft) scarp of the East Cache fault zone, in the Logan Country Club golf course, Logan, Utah. Trench logging was performed by James P. McCalpin and L.C. Allen Jones on April 5 and 6, 1991. Unit descriptions were made by James P. McCalpin. Three major depositional units are recognized (from oldest to youngest, units 1, 2, and 3), some of which are subdivided as noted by lower-case letters. Two younger soil horizons (A1, A2) are superimposed on some units.

Unit 1- Alluvial terrace deposit of the Logan River (predates formation of the fault scarp)

- Unit 1a-** 10YR7/3, cobble and pebble gravels in sparse medium to coarse sand matrix; maximum diameter 30 centimeter (12 in), average diameter 8 to 10 centimeters (3-4 in); moderately well sorted; subround; CaCO₃ coats are generally absent on stones; poor stratification; minor sand lenses indicate gentle west dip; at least 60 centimeters (24 in) thick; old photographs indicate unit is underlain by about 2.8 meters (9.2 ft) of similar-appearing cobbly strath terrace gravel (figure 5, this paper); organic horizon of the modern soil (soil A2) is developed on this unit on the upthrown fault block.
- Unit 1b-** 10YR7/2, pebble gravel in a sparse, medium to coarse sand matrix; maximum diameter 15 centimeters (6 in), average diameter 5 to 8 centimeters (2-3 in); moderately well sorted; subround; some openwork gravel, clasts 3 to 5 centimeter (1.2-2 in) diameter; CaCO₃ coats on bottoms of all stones, extending up the sides of about 50 percent of stones (Stage I+ carbonate); in places CaCO₃ coats do not extend to basal contact of unit 1b (see hachured lines on figure 5); irregular erosional contact into underlying unit 1a.
- Unit 1c-** 10YR6/3, pebble and cobble gravel in a matrix of abundant silt and fine sand; maximum diameter 25 centimeters (10 in), average diameter 10 centimeters (4 in); subround-subangular; poorly sorted; CaCO₃ coats on bottoms of some stones; irregular, interfingering contact with underlying unit 1b; probably a thin debris flow.

Unit 2- Earlier colluvium and sag pond (?) deposit (deposited soon after faulting event)

- Crack fill-** 10YR5/4, loose pebble and cobble gravel in a friable sand matrix; maximum diameter 20 centimeters (8 in), average diameter 10 centimeters (4 in); poorly sorted; subangular-subround; open void spaces between stones; abundant small rootlets follow void spaces; clast long axes steeply inclined to west; position of CaCO₃ coats on left sides of stones suggest coats were formed when clasts were horizontal in unit 1b, and then were subsequently rotated when clasts fell into basal tension fissure from free face; sharp, steep contacts with units 1a and 1b; basal radiocarbon age of 3,100 ± 80 yr B.P. (Beta-48112) on sandy, organic matrix is younger than age of overlying units 2a and 2b, and is probably contaminated by rootlets.
- Unit A1/2a-** 10YR4/2, silty sand with rare "floating" pea gravel clasts; massive, no visible stratification; the depositional unit 2a is probably a thin slopewash deposit formed in a scarp-base sag; 2a has been overprinted with organic matter accumulation from soil A1; this unit interfingers with basal debris-facies colluvium shed from scarp (unit 2b); radiocarbon age on silty organic soil matrix in upper half of unit is 4,040 ± 60 yr B.P. (Beta-48114).
- Unit 2b-** 10YR5/2, pebble gravel in a matrix of organic sand and silt; maximum diameter 12 centimeters (4.7 in), average diameter 5 to 8 centimeters (2-3 in); moderately well sorted; subround; consistent clast fabric, with clast long axes plunging about 25 degrees west; unconformably overlies crack fill, in which typical clast long axes plunge 60 to 75 degrees west; organic matter uniformly dispersed in matrix was presumably derived from soil A horizon exposed in scarp free face; basal radiocarbon age of 4,240 ± 80 yr B.P. (Beta-48113) from organic sandy matrix.

Unit 3- Later wash-facies colluvium (deposited after disappearance of scarp free face, to present)

- Unit A2/3-** 10YR4/4, silty sand with abundant "floating" pebbles; massive, no visible stratification; conformably overlies units 2b and A1/2a; represents a fine-grained, wash-facies colluvium (partly eolian loess?) with superimposed cumulic organic soil development (soil A2).